



**Sediment Micromorphology and Site Formation Processes
During the Middle to Later Stone Ages at the Haua Fteah
Cave, Cyrenaica, Libya**

Journal:	<i>Geoarchaeology</i>
Manuscript ID	GEO-16-108.R1
Wiley - Manuscript type:	Research Article
Date Submitted by the Author:	n/a
Complete List of Authors:	Inglis, Robyn Helen; University of York, Archaeology; Macquarie University, Environmental Sciences French, Charles; University of Cambridge, Archaeology Farr, Lucy; University of Cambridge, McDonald Institute for Archaeological Research Hunt, Chris; Liverpool John Moores University, Natural Sciences and Psychology Jones, Sacha; University of Cambridge, McDonald Institute for Archaeological Research Reynolds, Tim; Birkbeck, History Classics & Archaeology Barker, Graeme; University of Cambridge, McDonald Institute for Archaeological Research
Keywords:	Cave Sediments, Site Formation Processes, North Africa, Palaeolithic Archaeology, Sediment Micromorphology

1
2
3 **Sediment Micromorphology and Site Formation Processes During the Middle to**
4
5 **Later Stone Ages at the Haua Fteah Cave, Cyrenaica, Libya**
6
7

8
9
10 Robyn H. Inglis

11 Department of Archaeology, University of York, UK; Department of Environmental
12 Sciences, Macquarie University, Australia
13

14
15 Charles French

16
17 Department of Archaeology and Anthropology, University of Cambridge, UK
18
19

20
21 Lucy Farr

22 McDonald Institute for Archaeological Research, University of Cambridge, UK
23
24

25
26 Chris O. Hunt

27 School of Natural Sciences and Psychology, Liverpool John Moores University, UK
28
29

30
31 Sacha C. Jones

32 McDonald Institute for Archaeological Research, University of Cambridge, UK
33
34

35 Tim Reynolds

36 Department of History, Classics and Archaeology, Birkbeck, University of London,
37 UK
38
39

40
41 Graeme Barker

42 McDonald Institute for Archaeological Research, University of Cambridge, UK
43
44
45
46
47
48
49
50
51
52
53
54
55
56
57
58
59
60

ABSTRACT

Understanding the timing, conditions and characteristics of the Middle to Later Stone Age (MSA/LSA) transition in North Africa is critical for debates regarding the evolution and past population dynamics of *Homo sapiens*, especially their dispersals within, out of, and back into, Africa. As with many cultural transitions during the Palaeolithic, our understanding is based predominantly on archaeological and palaeoenvironmental records preserved within a small number of deep cave sediment sequences. To use such sequences as chronological cornerstones we must develop a robust understanding of the formation processes that created them. This paper utilises geoarchaeological analyses (field observations, sediment micromorphology, bulk sedimentology) to examine site formation processes and stratigraphic integrity during the MSA/LSA at the Haua Fteah cave, Libya, one of North Africa's longest cultural sequences. The depositional processes identified vary in mode and energy, from aeolian deposition/reworking to mass colluvial mudflows. These changing processes impact greatly on the interpretation of the palaeoenvironmental and archaeological records, not least in identifying potential colluvial sediment deposition and reworking in layers identified as containing the MSA/LSA transition. This study highlights the importance of developing geoarchaeological analyses of cultural sequences to fully unravel the limitations and potential of their contained archaeological and palaeoenvironmental records.

KEY WORDS: Sediment Micromorphology; Geoarchaeology; Caves; North Africa; Site Formation Processes.

INTRODUCTION

The appearance of Later Stone Age (LSA) stone tool industries within Africa after ca. 50,000 years BP (ca. 50 ka) marked a major change in human behaviour, contrasting starkly with the behavioural practices of the Middle Stone Age (MSA, Barham & Mitchell 2008). The mechanisms, conditions and chronologies of the development of LSA industries from the MSA industries that preceded them are the subject of intense debate, as summarised by authors in Jones and Stewart (2016). Even polarising archaeological entities into neat conceptual ‘blocks’ — MSA or LSA — can be problematic, ignoring both variation in and the fluid nature of human behaviour (Mitchell, 2016: 409). The North African archaeological record is central to these debates. Given its location between Sub Saharan Africa and the Levant, North Africa is a region crucial to understanding the dispersals of *Homo sapiens* populations (‘modern humans’) out of as well as back into Africa (Foley and Lahr 1997; Garcea, 2012, 2016; Van Peer, 1998). Establishing the timing and palaeoenvironments of the MSA/LSA transition across this key region is critical if we are to reveal past population histories in North Africa, yet our understanding of this important transition still requires clarification (Barton et al., 2016). Although arguments concerning the MSA/LSA transition in North Africa have mostly centred on population dispersal scenarios, it currently remains unclear to what extent such a technological shift may reflect: 1) migrations into new regions of human populations using culturally and technologically distinct tool kits (Oliveri et al., 2006; Pereira et al., 2010); 2) *in situ* technological adaption to changing environmental conditions and resources (Garcea,

1
2
3
4 2010); 3) a change in population dynamics and enhanced opportunities for cultural
5
6 transmission (Powell et al., 2009); 4) a biological change occurring in human populations
7
8 (Klein, 1994); or 5) a combination of these scenarios, such as decreasing residential mobility,
9
10 population growth and environmental change (Tryon & Faith, 2016).
11
12

13
14
15 Present understanding of the MSA/LSA transition in North Africa is, as in the case of most
16
17 Palaeolithic regional chronologies, based largely on artefacts, palaeoenvironmental proxies and
18
19 dating material preserved within cave sediment sequences. Yet each of these stratigraphies
20
21 were formed through processes unique to their setting and history (Farrand, 2001; Woodward
22
23 & Goldberg, 2001). Changing modes and rates of deposition have been long known to impact
24
25 on the taphonomy of the archaeological record through sediment removal and reworking, or
26
27 changing rates of sedimentation and hiatuses (e.g. Butzer, 1971; Harris, 1989; Stein, 1987,
28
29 2001). This can distort interpretation of these cultural and environmental chronologies, and
30
31 create apparently abrupt changes in environmental proxies and/or technological artefact
32
33 attributes, as well as 'inversions' of cultural material (Campy & Chaline, 1993; Hunt et al.,
34
35 2015; Mallol et al., 2012). Therefore, if we are to use deep cave sequences as the cornerstones
36
37 of regional cultural chronologies, we must understand the processes that created them, and
38
39 consider the archaeological records they contain in light of this understanding.
40
41
42
43
44
45
46
47
48
49
50
51

52
53 Geoarchaeological analyses are well-placed to analyse site formation processes through a
54
55 range of methods and analytical scales (e.g. Bailey and Woodward 1997; Frumkin et al., 2016;
56
57
58
59
60

1
2
3
4 Mallol et al., 2009). In particular, sediment micromorphology allows microscopic interrogation
5
6
7 of sediments, enhancing field observations and complementing quantitative sediment analysis
8
9
10 (Goldberg & Sherwood, 2006; Woodward & Goldberg, 2001), especially in studies of
11
12 sedimentation rates and stratigraphic integrity beyond the reach of radiocarbon dating (e.g.
13
14
15 Aldeias et al., 2014; Karkanas & Goldberg, 2010; Mallol et al., 2012).
16
17

18
19 This paper utilises a range of geoarchaeological techniques to examine site formation
20
21 processes in the late MSA to early LSA layers at the Haua Fteah cave on the Cyrenaican coast
22
23 of northeast Libya (22°3'5"E, 32°53'70"N). The cultural sequence revealed by Charles
24
25
26
27
28
29
30
31
32
33
34
35
36
37
38
39
40
41
42
43
44
45
46
47
48
49
50
51
52
53
54
55
56
57
58
59
60
Renewed investigations by a multi-disciplinary team, The Cyrenaican Prehistory Project
(CPP), between 2007 and 2015 have combined archaeological excavation with
palaeoenvironmental and chronological analyses (e.g. Barker et al., 2007, 2008, 2009, 2010,
2012; Farr et al., 2014; Rabett et al., 2013). The present study, part of that project, combines
sediment micromorphology, bulk sedimentology, and field observations to develop a
sedimentological and taphonomic framework for the sediments containing the late MSA and
early LSA artefacts. Within this framework, the existing and existing and emerging

1
2
3
4 archaeological and palaeoenvironmental records of this important cultural sequence can be
5
6
7 situated and interpreted.

10 **THE MSA AND LSA IN NORTH AFRICA**

11
12 Reviews of the MSA and LSA of North Africa reveal a complexity of demographic
13
14 scenarios that may underlie the equally complex cultural shifts that occurred both within the
15
16 MSA and LSA and from the MSA to the LSA (Garcea, 2016; Van Peer, 2016). Population
17
18 movements during this period have often been linked to periods of climate change and
19
20 consequential ecological change (Timmerman & Friedrich, 2016). During humid episodes in
21
22 MIS 5 (ca. 130–71 ka), for example, populations with MSA technologies exploited a network
23
24 of rivers and lakes that traversed the Sahara (Drake & Breeze, 2016; Drake et al., 2013; Geyh
25
26 & Thiedig, 2008; Osborne et al., 2008). In contrast, arid conditions from MIS 4 (ca. 71–57 ka)
27
28 to MIS 2 (ca. 29–14 ka) — albeit with shorter humid periods during intervening MIS 3
29
30 (Hoffmann et al., 2016; Giraudi, 2005; Tjallingii et al., 2008) — are argued to have forced
31
32 populations to contract to the edges of the continent (Ambrose, 1998, 2003; Garcea, 2012), or
33
34 to small yet viable areas of the Nile valley (Van Peer et al., 2010: 241; Vermeersch & Van
35
36 Neer, 2015).
37
38
39
40
41
42
43
44
45
46
47
48
49

50 At this time when these late Pleistocene climatic changes were profoundly shaping
51
52 environments and landscapes in North Africa, LSA technologies appeared in various
53
54 archaeological records at various times. It is currently unclear whether the LSA assemblages
55
56
57
58
59
60

1
2
3
4 preserved within North African sequences represent diverse local trajectories and responses to
5
6
7 local environments during the Late Pleistocene, or movements of populations themselves,
8
9
10 within, out of, or back into Africa (Barham & Mitchell, 2008; Barton et al., 2016; Garcea,
11
12 2016). Our understanding is hampered by a lack of archaeological sites with deposits dating to
13
14
15 MIS 3 (ca. 57–29ka) when the MSA/LSA transition occurred in certain areas of North Africa
16
17
18 (Barham & Mitchell 2008; Barton et al. 2016). The Central Sahara and Western Desert of
19
20
21 Egypt are argued to have been abandoned after MSA occupation, and remaining so until the
22
23
24 Holocene (Barham & Mitchell, 2008: 265; Garcea 2004, 2012; Garcea and Giraudi 2006; Jones
25
26
27 et al., 2016) although evidence from the Central Sahara suggests that the presence of
28
29
30 populations in the region with LSA technologies during MIS 3/2 cannot be excluded as a
31
32
33 possibility (Cancellieri et al., 2016: 142). The Nile Valley, an area that potentially preserved
34
35
36 localised refuges from Saharan aridity, reveals the presence of artefacts of the ‘Khaterian’
37
38
39 complex at Nazlet Khater. These date from from 40–32ka (Vermeersch 2010) and suggest that
40
41
42 LSA industries developed locally from the MSA, potentially driven by growing environmental
43
44
45 and population pressures (Van Peer & Vermeersch, 2007). Likewise, whilst sites in the
46
47
48 Maghreb may have been subject to sporadic abandonment, at Grotte des Pigeons (Taforalt), the
49
50
51 cultural sequence appears to contain a series of stepped, local changes in technology between
52
53
54 the MSA and LSA (Barton et al., 2016). The MSA/LSA transition is, however, later in the
55
56
57 Maghreb than the Nile Valley, with the earliest LSA Iberomaurusian dated to 25–23ka (Barton
58
59
60

1
2
3
4 et al., 2013). Situated between these two potential refuges, lies the MSA/LSA sequence at the
5
6
7 Haua Fteah, where the transition from the MSA to the LSA 'Early Dabban' industries has been
8
9
10 dated to 46–41 ka (Barton et al., 2015; Douka et al., 2014). This site occupies a central position
11
12
13 in understanding the potential cultural connections and local trajectories of this important
14
15
16 cultural shift.

17 18 **THE HAUA FTEAH MSA/LSA SEQUENCE** 19

20
21 The Haua Fteah cave is a semi-collapsed karstic phreatic cave on the northern escarpment of
22
23 the Gebel Akhdar ('Green Mountain') limestone massif in Northeast Libya. The Gebel Akhdar
24
25 (Figure 1) covers an area ~300 x 400 km and rises in series of three escarpments to over 800 m
26
27 (McBurney & Hey, 1955). Its topography and position in the path of Mediterranean Westerlies
28
29 cause it to receive more rainfall than the surrounding regions - ~800 mm per year compared to
30
31 ~250 mm for the surrounding regions (Libyan National Meteorological Centre). The cave is ~1
32
33 km from the present shoreline and ~63 m asl, with a mouth ~80 m wide and ~20 m high. The
34
35 floor of the cave consists of bare, largely dry, silty sediment which is easily mobilised by the
36
37 wind and wetted in small areas by dripping from the cave roof. The floor remains largely dry
38
39 during rain, yet runoff from intense storms can transport significant volumes of sediment and
40
41 soil into the cave (Hunt et al., 2010).
42
43
44
45
46
47
48
49
50
51

52
53 The massif was connected to Saharan rivers and lakes during MIS 5 (Drake & Breeze, 2016;
54
55
56 Drake et al., 2013; Geyh & Thiedig, 2008; Osborne et al., 2008) and it probably acted as a
57
58
59
60

1
2
3
4 refuge during glacial periods (Klein & Scott, 1986; McBurney & Hey, 1955; Prendergast et al.,
5
6
7 2016; Reade et al., 2016). The Mediterranean coastline and the marine resources it contained
8
9
10 may have increased the area's attractiveness to hominin populations, as well as providing a
11
12
13 corridor for dispersal (Bailey & Flemming, 2008). The region's steep offshore topography
14
15
16 means that the position of the coastline in the immediate vicinity is unlikely to have receded
17
18
19 more than 3 km during peak glacial conditions (Lambeck & Purcell, 2005; GEBCO_14).

20
21 The location and long cultural sequence of the Haua Fteah make it pivotal to understanding
22
23
24 prehistoric cultural change in North Africa. The 1950s excavations revealed ~14 m of deposits
25
26
27 containing cultural materials from the MSA to the historic period (McBurney, 1967).
28
29
30 McBurney excavated in three stepped, inset trenches named by the present project, which
31
32
33 emptied the McBurney trench of the 1955 backfill: the Upper Trench (from the ground surface
34
35
36 to ~2 m depth), the Middle Trench (~2–7 m), and the Deep Sounding (~7–14 m). McBurney
37
38
39 excavated in spits that often cross-cut sediment layers, though the relationship of the spits to
40
41
42 stratigraphic layers was observed as the excavation proceeded downwards (McBurney, 1967).
43
44
45 The present project has excavated new areas alongside McBurney's trench in the Upper and
46
47
48 Middle Trenches, as well as the Deep Sounding where excavations extended a further ~1 m
49
50
51 below the base of McBurney's excavations. Of primary interest to the work presented here is
52
53
54 the ~2.0 x 1.0 m trench (Trench M) and a 0.3 x 0.3 m sample column alongside the Middle
55
56
57
58
59
60

1
2
3
4 Trench, as well as two 0.3 x 0.3 m sample columns excavated down the West- and North-
5
6
7 Facing Profiles (see below).

8
9
10 Using the Middle Palaeolithic (MP) and Upper Palaeolithic (UP) terminologies of Europe
11
12 and the Near East, McBurney classified the earliest industry, a flake- and blade-based MSA
13
14 industry, as 'Libyan Pre-Aurignacian MP'. It occurred in three concentrations within the Deep
15
16 Sounding (McBurney, 1967), with occasional lithics and shell fragments recovered throughout
17
18 the Deep Sounding (Farr et al., 2014; McBurney, 1967; Rabett et al., 2013). These sediments
19
20 have been dated by Optically Stimulated Luminescence (OSL) to MIS 5, with the base of the
21
22 sequence lying below the MIS 5/6 boundary (Jacobs et al., 2017). Close to the base of the
23
24 Middle Trench, artefacts with 'Levallois-Mousterian MP' affinities were found by McBurney
25
26 in initially high numbers from sediments for which the present project, using new ¹⁴C and OSL
27
28 determinations, has provided a modelled age of 75–70 ka (Douka et al., 2014). These levels
29
30 yielded two *Homo sapiens* mandibles at first regarded as 'Neanderthaloid' (McBurney, 1967;
31
32 McBurney et al., 1952, 1953; Tobias, 1967; Trevor and Wells, 1967) but since recognised as
33
34 fully modern human (Hublin, 1991, 2001). Artefact numbers then dropped significantly,
35
36 remaining low into McBurney's Layer XXV, which he identified as containing the first UP (i.e.
37
38 LSA) industry at the site, which he termed 'Dabban' because he had found similar material in
39
40 the nearby cave of Hagfet ed-Dabba a few years previously (McBurney, 1967; McBurney and
41
42 Hey 1955). Tephra shards identified as the Campanian Ignibrite/Y5 tephra, (dated to 39.28 ±
43
44
45
46
47
48
49
50
51
52
53
54
55
56
57
58
59
60

1
2
3
4 0.11 ka BP, De Vito et al., 2001) were found associated with the contact between Context 441
5
6
7 and 442 (Figure 4) in Early Dabban layers (Barton et al., 2015; Douka et al., 2014), and were
8
9
10 included in the Bayesian model which produced a modelled age of 46–41 ka for the deposition
11
12 of the Dabban layers (Douka et al., 2014), a date consistent with the earliest UP industries of
13
14 the Levant and Europe (Benazzi et al., 2011; Higham et al., 2011; Rebollo et al., 2011).
15
16
17 Genetic evidence suggests a migration of Levantine populations into North Africa at this time
18
19 (Olivieri et al., 2006), perhaps along the Mediterranean coastline.
20
21
22
23

24 The nature of the MSA/LSA transition at the Haua Fteah, as understood from the 1950s
25
26 excavations, is unclear. It is compounded by very low artefact densities in Layer XXV (as well
27
28 as in the immediately underlying and overlying layers) and is complicated by the fact that this
29
30 layer, which was subdivided into sub-units a–e, produced Levalloiso-Mousterian material in
31
32 XXVc overlying the appearance of potentially LSA Dabban material in XXVd (McBurney
33
34 1967: 138). Similar complexity is emerging from the initial analysis of the small number of
35
36 finds located at these depths by the new stratigraphic excavations (Farr et al., 2014; Rabett et
37
38 al., 2013). The potential interstratification of MSA and LSA technologies observed by
39
40
41
42
43
44
45
46
47
48
49
50
51
52
53
54
55
56
57
58
59
60
61
62
63
64
65
66
67
68
69
70
71
72
73
74
75
76
77
78
79
80
81
82
83
84
85
86
87
88
89
90
91
92
93
94
95
96
97
98
99
100
101
102
103
104
105
106
107
108
109
110
111
112
113
114
115
116
117
118
119
120
121
122
123
124
125
126
127
128
129
130
131
132
133
134
135
136
137
138
139
140
141
142
143
144
145
146
147
148
149
150
151
152
153
154
155
156
157
158
159
160
161
162
163
164
165
166
167
168
169
170
171
172
173
174
175
176
177
178
179
180
181
182
183
184
185
186
187
188
189
190
191
192
193
194
195
196
197
198
199
200
201
202
203
204
205
206
207
208
209
210
211
212
213
214
215
216
217
218
219
220
221
222
223
224
225
226
227
228
229
230
231
232
233
234
235
236
237
238
239
240
241
242
243
244
245
246
247
248
249
250
251
252
253
254
255
256
257
258
259
260
261
262
263
264
265
266
267
268
269
270
271
272
273
274
275
276
277
278
279
280
281
282
283
284
285
286
287
288
289
290
291
292
293
294
295
296
297
298
299
300
301
302
303
304
305
306
307
308
309
310
311
312
313
314
315
316
317
318
319
320
321
322
323
324
325
326
327
328
329
330
331
332
333
334
335
336
337
338
339
340
341
342
343
344
345
346
347
348
349
350
351
352
353
354
355
356
357
358
359
360
361
362
363
364
365
366
367
368
369
370
371
372
373
374
375
376
377
378
379
380
381
382
383
384
385
386
387
388
389
390
391
392
393
394
395
396
397
398
399
400
401
402
403
404
405
406
407
408
409
410
411
412
413
414
415
416
417
418
419
420
421
422
423
424
425
426
427
428
429
430
431
432
433
434
435
436
437
438
439
440
441
442
443
444
445
446
447
448
449
450
451
452
453
454
455
456
457
458
459
460
461
462
463
464
465
466
467
468
469
470
471
472
473
474
475
476
477
478
479
480
481
482
483
484
485
486
487
488
489
490
491
492
493
494
495
496
497
498
499
500
501
502
503
504
505
506
507
508
509
510
511
512
513
514
515
516
517
518
519
520
521
522
523
524
525
526
527
528
529
530
531
532
533
534
535
536
537
538
539
540
541
542
543
544
545
546
547
548
549
550
551
552
553
554
555
556
557
558
559
560
561
562
563
564
565
566
567
568
569
570
571
572
573
574
575
576
577
578
579
580
581
582
583
584
585
586
587
588
589
590
591
592
593
594
595
596
597
598
599
600
601
602
603
604
605
606
607
608
609
610
611
612
613
614
615
616
617
618
619
620
621
622
623
624
625
626
627
628
629
630
631
632
633
634
635
636
637
638
639
640
641
642
643
644
645
646
647
648
649
650
651
652
653
654
655
656
657
658
659
660
661
662
663
664
665
666
667
668
669
670
671
672
673
674
675
676
677
678
679
680
681
682
683
684
685
686
687
688
689
690
691
692
693
694
695
696
697
698
699
700
701
702
703
704
705
706
707
708
709
710
711
712
713
714
715
716
717
718
719
720
721
722
723
724
725
726
727
728
729
730
731
732
733
734
735
736
737
738
739
740
741
742
743
744
745
746
747
748
749
750
751
752
753
754
755
756
757
758
759
760
761
762
763
764
765
766
767
768
769
770
771
772
773
774
775
776
777
778
779
780
781
782
783
784
785
786
787
788
789
790
791
792
793
794
795
796
797
798
799
800
801
802
803
804
805
806
807
808
809
810
811
812
813
814
815
816
817
818
819
820
821
822
823
824
825
826
827
828
829
830
831
832
833
834
835
836
837
838
839
840
841
842
843
844
845
846
847
848
849
850
851
852
853
854
855
856
857
858
859
860
861
862
863
864
865
866
867
868
869
870
871
872
873
874
875
876
877
878
879
880
881
882
883
884
885
886
887
888
889
890
891
892
893
894
895
896
897
898
899
900
901
902
903
904
905
906
907
908
909
910
911
912
913
914
915
916
917
918
919
920
921
922
923
924
925
926
927
928
929
930
931
932
933
934
935
936
937
938
939
940
941
942
943
944
945
946
947
948
949
950
951
952
953
954
955
956
957
958
959
960
961
962
963
964
965
966
967
968
969
970
971
972
973
974
975
976
977
978
979
980
981
982
983
984
985
986
987
988
989
990
991
992
993
994
995
996
997
998
999
1000

1
2
3
4 emerging new archaeological data from the entire sequence within a solid model of formation
5
6
7 processes.

10 **THE HAUA FTEAH SEDIMENT SEQUENCE**

13 Basic sediment analysis and interpretation of the Haua Fteah sequence were undertaken
14
15 during the 1950s excavations, and a broad framework for understanding the modes of
16
17 sedimentation developed (McBurney 1967; Sampson, 1967). Layers of limestone gravel and
18
19 sand in the Haua Fteah sediments were interpreted as likely weathered from the cave roof
20
21 (Sampson, 1967), during periods of cooling and increased physical weathering (now correlated
22
23 with MIS 4, MIS 2; Douka et al., 2014). Deposition of fine material was attributed to wind and
24
25 water action (McBurney, 1967) in warmer phases such as the the Eemian (now correlated to
26
27 MIS 5, MIS 3; Douka et al., 2014). Moyer (2003) later posited that these fine sediments were
28
29 the result of inwash during pluvials. These interpretations were, however, based solely on field
30
31 observations and coarse material measurement, and in particular the deposition mechanisms of
32
33 fine material remained untested.
34
35
36
37
38
39
40
41
42
43
44

45 As part of the renewed excavations, the sediment sequence was divided into five facies
46
47 reflecting differences in the dominant site formation processes (Douka et al., 2014; Inglis,
48
49 2012) (Figures 3 and 4). Three fine-grained facies (Facies 1, 3 and 5) were separated by two
50
51 dominated by limestone gravel and sand (Facies 2 and 4). Field observations during the new
52
53 fieldwork, followed by bulk sedimentological studies, interpreted the silty layers within Facies
54
55
56
57
58
59
60

1
2
3
4 1 as deposited by inwash and mudflow events that were interleaved with heavily
5
6 anthropogenically-influenced sediments and debris-avalanche deposits from roof-collapse
7
8
9
10 (Hunt et al., 2010). Modelling of radiocarbon-dated shell fragments, and interpretation of
11
12 palynological analyses and field descriptions, extended this 'sump' model into the upper part of
13
14
15 Facies Two, where sediments were interpreted as predominantly debris flows (Hunt et al.,
16
17
18 2015).

20 **METHODS**

21
22 This paper presents the analysis of the sediments, and the interpretation of the processes that
23
24 deposited them, in the 'Levalloiso-Mousterian' MSA and 'Early Dabban' LSA layers in the
25
26 Middle Trench: Facies 3, 4 and the top part of Facies 5, which were the subject of RHI's PhD
27
28 (Inglis, 2012). A multi-scalar geoarchaeological approach was employed: field descriptions
29
30 were combined with high-resolution soil micromorphological analysis of each context, while
31
32 bulk sedimentological analyses on the <2 mm fraction provided measurement of the fine
33
34 sediment properties. In addition, two soil pits in the local *terra rossa* were dug and sampled to
35
36 provide modern analogues, Pit R directly upslope of the cave opening and 5 m from the lip of
37
38 the roof (two small bulk samples collected), and Pit T, located on the slopes below the cave, ~
39
40 200 m to the NNW of the Haua Fteah (three small bulk).
41
42
43
44
45
46
47
48
49
50

51
52 **Field Observations** After removal of the backfill and cleaning the 1950s sections, the
53
54 excavators used the single context system (MOLAS, 1994) to record discrete sediment layers
55
56 defined by several key field characteristics, e.g., colour, texture of fine and coarse material,
57
58
59
60

1
2
3
4 shape, and clast orientation. Use of context divisions in sampling for sedimentological,
5
6
7 micromorphological and palaeoenvironmental analyses ensured that data could be correlated
8
9
10 with archaeological assemblages from each context as excavations progressed.

11
12 **Sediment Micromorphology** Sediment micromorphological sampling was undertaken of
13
14
15 the majority of contexts on the West-Facing Profile in Facies 5–3, as well as corresponding
16
17
18 North-Facing Profile contexts in areas of variable stratigraphy and at the depth of McBurney's
19
20
21 Layer XXV (Figure 4). Sampling focused on upper and lower contacts of each context to
22
23
24 characterise the mode of deposition, material within each deposit and the transitions between
25
26
27 them. Intact sediment blocks were removed from profiles using Kubiena tins or foil food
28
29
30 containers, and secured with tissue paper and parcel tape to allow drying in the field before
31
32
33 wrapping in clingfilm for transport. Blocks were air-, then oven-dried for 48 hours prior to
34
35
36 impregnation with crystallitic polymer resin under vacuum, following capillary rise. Thirteen ×
37
38
39 7 cm or 7 × 5 cm slices were cut from cured blocks and ground to 30µm using a Brot
40
41
42 multiplate grinding machine. Thin-sections were examined by eye and using a Leica Wild M40
43
44
45 wide-view microscope (×4 to ×35 magnification), and a Leitz Laborlux 12 Pol microscope
46
47
48 (×40 to ×400 magnification), under plane polarized (PPL), crossed polarized (XPL), and
49
50
51 oblique incident light (OIL). Description followed Bullock et al. (1985), Courty et al. (1989),
52
53
54 and Stoops (2003). Micro-fabrics within each slide were defined on the basis of changes in
55
56
57 micromorphological characteristics within a sample, and numbered in stratigraphic order from
58
59
60

1
2
3
4 the top of the slide. For example, Micro-Fabric 2521:1 overlies 2521:2 and is the uppermost
5
6
7 unit in the slide made from Sample 2521 (the sample number was assigned in the Haua Fteah
8
9
10 environmental sample register).

11
12 **Bulk Sediment Analyses** Sample columns (30 × 30 cm) were excavated through Facies 3–5
13
14
15 sediments on the North- and West-Facing Profiles (Figure 4). Samples at 5 cm intervals
16
17
18 respecting context boundaries were collected for bulk sedimentological analyses, as well as
19
20
21 palynology, phytolith analysis and tephrochronology (e.g. Barton et al., 2015; Douka et al.,
22
23
24 2014; Simpson, 2014). The <2 mm fraction was analysed for: particle size distributions,
25
26
27 percent loss on ignition organics (%LOI organics), percent carbonate (%CaCO₃), and magnetic
28
29
30 susceptibility. For the particle size analysis alone, carbonates were removed from the sample
31
32
33 prior to analysis (see next section); all other bulk sedimentological analyses were carried out
34
35
36 on the complete <2mm fraction.

37
38 **Laser particle size analysis** of the 0.02–2000 µm sediment fraction can distinguish a
39
40
41 sediment's transport method or source (Folk, 1966; Pye & Blott, 2004), potentially useful at the
42
43
44 Haua Fteah for distinguishing between colluvially- and aeolian-transported sediments. Given
45
46
47 that the limestone from the cave left <1% residue after dissolution (Inglis, 2012), the volume of
48
49
50 limestone required to produce this would be far greater than that dissolved in the formation of
51
52
53 the cave. The non-carbonate fraction in the Haua Fteah sediments was therefore considered to
54
55
56 be predominantly allochthonous. Removal of carbonates was therefore undertaken to avoid
57
58
59
60

1
2
3
4 concretion of sediment particles by carbonate precipitated in the cave, and to examine the
5
6 allochthonous, non-carbonate source of the material. It is noted, however, that this would also
7
8 remove purely allochthonous carbonate material (if present), although it would be expected
9
10 that such variation in lithology, if of a sufficient magnitude, would be visible in the
11
12 micromorphological observations. The processes may also remove phytoliths from the sample,
13
14 altering the silt fraction in the non-carbonate PSD. Samples were treated overnight with 10%
15
16 HCl, and dispersed in 4.4% sodium pyrophosphate and distilled water. Analysis was carried
17
18 out using a Malvern Mastersizer 2000, and the ultrasonic probe used throughout measurement
19
20 to ensure clay deflocculation. Samples were measured three times for 30 s, and the average
21
22 distribution taken. Measurement was repeated until the curve stabilised.
23
24
25
26
27
28
29
30
31
32

33 *%LOI organics.* Raised organic content of sediments may indicate anthropogenic activity
34
35 (e.g. Macphail et al., 2004; Sánchez Vizcaíno & Cañabate, 1999; Stein, 1992) or palaeosol
36
37 formation (Ellis & Mellor, 1995). %LOI organics was determined by heating pre-weighed,
38
39 dried samples to 425°C for 24 hours and, on cooling, noting the mass lost.
40
41
42
43
44

45 *%CaCO₃* in limestone cave sediments originates from multiple sources: limestone roof-spall
46
47 from physical weathering (Laville, 1976), carbonate-rich source material (e.g. aeolian sources,
48
49 Coudé-Gaussen & Rognon, 1993), precipitation from carbonate-rich water (White, 2007) or
50
51 ash (Canti 2003). These different depositional processes highlight the need for bulk %CaCO₃
52
53
54
55
56
57
58
59
60

1
2
3
4 to be interpreted in the context of field and micromorphological observations. %CaCO₃
5
6
7 contents were determined through calcimetry following Gale and Hoare (1991).
8
9

10 ***Magnetic Susceptibility*** serves as a measure of ferro- or ferrimagnetic materials within a
11
12 sample (Thompson & Oldfield, 1986), the concentration of which can be raised or lowered
13
14 through changes in redox conditions through burning, waterlogging, wetting and drying cycles,
15
16 or biological activity (Sternberg, 2001). Variation in magnetic susceptibility may also mark
17
18 variation in source material, and magnetic susceptibility variability of re-deposited soils has
19
20 been used in caves as a proxy for external environmental conditions (e.g. Ellwood et al., 2004),
21
22 although this latter interpretation did not take into account the multiple mechanisms that may
23
24 raise magnetic susceptibility, including burning (Tite & Mullins, 1971). The low frequency
25
26 magnetic susceptibility of the samples was measured using a Bartington MS2B Meter.
27
28
29
30
31
32
33
34
35

36 **RESULTS**

37 **Micromorphological and Field Observations**

38
39
40
41 The three MSA and LSA facies are described from the base of the Middle Trench upwards.
42
43 Interpreted site formation processes and bulk sedimentological variables are summarised by
44
45 context in Figure 5. For summary micromorphological descriptions, refer to Supplementary
46
47 Tables 1–5, and Inglis (2012) for full descriptions. All facies dates are modelled Bayesian age
48
49 ranges for deposition following Douka et al. (2014), and thus some overlap with adjacent
50
51 facies.
52
53
54
55
56
57
58
59
60

1
2
3
4 *Facies 5 (Middle Trench): ~ 75–65 ka*
5
6

7 Facies 5 (Contexts 528–520, West-Facing Profile; 538–521, North-Facing) in the Middle
8
9 Trench consists of red and orange silt layers, some of which crossed both profiles, interspersed
10
11 with combustion features and rare organic lenses. Some redder, more clayey layers lens out on
12
13 the West-Facing Profile towards the back wall of the cave (e.g. Context 520), indicating their
14
15 origin outside the cave mouth. Between Contexts 523 and 521 a series of small combustion
16
17 features were spaced across the South-, East- and West-Facing Profiles. Micromorphological
18
19 sampling covered Contexts 523–520 (West-Facing Profile) and 528–521 (North-Facing).
20
21 Micromorphological observations (Supplementary Table 1) showed a largely consistent fine
22
23 material composition of sandy silt/silt loams with micritic crystallitic to stipple-speckled b-
24
25 fabrics. Micro-fabrics throughout Facies 5 shifted between those that contained lenses of
26
27 material (fine sand, silt, or dung), and rarer micro-fabrics with more chaotic arrangements and
28
29 sharp lower boundaries. These variations occurred within, and between, contexts (e.g. Context
30
31 563). Occasional crust fragments were observed on both profiles, and calcite precipitation on
32
33 the West-Facing Profile (Context 521). Lenses of charcoal, ash and other charred and humified
34
35 material were observed throughout. Facies 5 was capped on the West-Facing Profile by a dark
36
37 red, clayey context (520) with a sharp lower boundary and stipple-speckled b-fabric (Micro-
38
39 Fabrics 2000:1).
40
41
42
43
44
45
46
47
48
49
50
51
52
53
54

55
56 *Facies 4 (Middle Trench): ~ 68–47ka*
57
58
59
60

1
2
3
4 Facies 4 (Contexts 517–513, West-Facing Profile; Contexts 567–513, North-Facing) was
5
6 characterised in the field by limestone gravel in a pale, friable orange to grey silty matrix. On
7
8 the North-Facing Profile it was capped by a combustion feature (Contexts 513 and 535) that
9
10 sloped down to the east. Only Context 513 continued across both profiles, grading from grey
11
12 on the North-Facing Profile to orange on the West-Facing. Micromorphologically
13
14 (Supplementary Table 2), the micro-fabrics in Facies 4 exhibited more distinct variation than
15
16 those in Facies 5. On the West-Facing Profile, Context 517 (516 was not sampled) is a pale,
17
18 limestone-dominated sandy silt loam/silt loam, with some dung lenses and a stipple
19
20 speckled/micritic crystallitic b-fabric (Micro-Fabrics 2666:1 & 2). Similar micro-fabrics were
21
22 observed on the North-Facing Profile, in layers of greyish, limestone-sand sandy silt loams
23
24 with horizontal orientation of the coarse material (e.g. Contexts 567, 536), sometimes
25
26 containing small red clayey stringers and crusts as well as calcitic hypocoatings. These micro-
27
28 fabrics were interstratified with lenses of redder sandy clay loams with interleaved/sharp lower
29
30 boundaries, indicating major variation in depositional energy and character. These layers are
31
32 capped by a large, weathered combustion feature (Contexts 535, 513) consisting of a series of
33
34 ash and phytolith-rich layers (Inglis, 2012), potentially formed by combustion of grass-rich
35
36 fuel (S. E. Jones, pers. comm. 2012).
37
38
39
40
41
42
43
44
45
46
47
48
49
50
51

52
53 *Facies 3 (Middle Trench): ~ 48–34ka*
54
55
56
57
58
59
60

1
2
3
4 Facies 3 (Contexts 509–440, West Facing Profile; Contexts 508–440 North-Facing Profile)
5
6
7 consisted of silt layers varying in the field in compactness, colour, and texture, with dense,
8
9
10 reddish layers of silty clay that stood proud of cleaned profiles interspersed with friable, pale
11
12 yellow and orange silt layers. On the West-Facing Profile, some layers (both silty and clayey)
13
14 were indurated by carbonate (e.g. Context 490). The horizontal layers largely continued across
15
16 both profiles. Gravel layers became thicker and more frequent towards the overlying, gravel-
17
18 dominated Facies 2. Facies 3 contained both MSA and LSA layers, separated by Layer XXV
19
20 which is argued to have contained interleaved MSA and LSA artefacts (McBurney, 1967). For
21
22 ease of discussion, description of the results for Facies 3 is divided here into sediment
23
24 characterised by these cultural artefacts.
25
26
27
28
29
30
31

32
33 The **Facies 3 MSA (“Levalloiso-Mousterian”) contexts (509–498)** (Supplementary Table
34
35 3) were commonly pale orange-brown and yellow silts with little limestone gravel, with a shift
36
37 towards a higher frequency of redder and more compact layers from Contexts 503–499, some
38
39 of which were restricted to the West-Facing profile, and lensing out towards the back wall of
40
41 the cave, indicating that they had originated from the cave mouth (e.g. Context 491). The
42
43 Facies 3 MSA layers were sampled for micromorphological analysis on the West-Facing
44
45 Profile only. Whilst containing less limestone sand and gravel than Facies 4, the
46
47 micromorphological observations of the fine material were consistent with the underlying
48
49 facies, that is, they varied between pale, sandy silt loams/silt loams containing dung lenses and
50
51
52
53
54
55
56
57
58
59
60

1
2
3
4 stringers of fine material and other, redder, clay loams/silty clay loams with chaotically-
5
6 arranged coarse material and clear lower boundaries that, in places, crossed both profiles (e.g.
7
8
9 Contexts 508, 499, 498). A third group contained chaotically-arranged pale silty loams with
10
11 micritic crystallitic to stipple-speckled b-fabrics (e.g. Contexts 506, 505). On the West-Facing
12
13 Profile, all contexts from the upper part of 505 to 498 contained calcitic hypocoatings or, as in
14
15 Context 503, micritic calcitic concretion of large areas of the groundmass.
16
17
18
19

20
21 **McBurney's Layer XXV** was defined from the 1950s section drawings as Contexts 497–
22
23 491 in the West-Facing Profile and Contexts 470–458 in the North-Facing Profile), covering a
24
25 greater depth than defined during excavation due to discrepancies on the published 1950s
26
27 profile drawings. Layer XXV contains markedly red, clayey layers that alternate with paler
28
29 silty layers. Those layers that were traceable across the two profiles were sampled on both. The
30
31 micromorphology of the Layer XXV contexts (Supplementary Table 4) was dominated by silt
32
33 loams/silty clay loams that contained fine material lamination, dung lenses and horizontal
34
35 orientation of coarse material, although Micro-Fabric 2521:2, the lower part of Context
36
37 494/459 on the North-Facing Profile, had a chaotic arrangement towards its base. Context
38
39 493/458 had a clear lower boundary and a similarly chaotic arrangement on both the West-
40
41 Facing Profile (Micro-Fabric 1014:2), and North-Facing Profile (Micro-Fabrics 2521:1,
42
43 2529:2), where it is redder. Context 491, restricted to the West-Facing Profile, was a reddish
44
45 silty clay loam with a clear lower boundary, and lensed out towards the back wall of the cave,
46
47
48
49
50
51
52
53
54
55
56
57
58
59
60

1
2
3
4 indicating it had originated in a movement from the cave entrance. Micritic calcitic void
5
6
7 hypocoatings were present in most West-Facing Profile contexts in Layer XXV.
8

9
10 **The Facies 3 LSA (“Dabban”) layers** (Contexts 490–236, West-Facing Profile; Contexts
11
12 455–202, North-Facing Profile) contained an increasing frequency of gravel lenses towards the
13
14 top (most prominent on the North-Facing Profile), interrupting otherwise red-orange silty
15
16 layers. The recorded stratigraphy varied between profiles, with some contexts on the West-
17
18 Facing Profile divided into finer layers on the North-Facing. Contexts 490–442 (West-Facing
19
20 Profile) and Contexts 547–461 (North-Facing Profile) were sampled for micromorphological
21
22 analysis. The LSA layers (Supplementary Table 5) were largely pale, silty loams/silty clay
23
24 loams with varying amounts of gravel and horizontal orientation to the fine and coarse material
25
26 as well as dung lenses, and occasional clay stringers and crusts. These contrasted with reddish
27
28 silty clay loams with sharp lower boundaries (Contexts 490, 461), some with reticulate b-
29
30 fabrics (e.g. Micro-Fabric 762:1, Context 461). Micro-Fabric 754A:2 in Context 453 is unique
31
32 in the Haua Fteah observations in that it contains distinct laminations and dung lenses as well
33
34 as mosaic and reticulate b-fabrics, dendritic manganese staining and semi-dissolved bone
35
36 associated with neoformed minerals. On the West-Facing Profile, some contexts were heavily
37
38 cemented by micritic calcite (e.g. Contexts 442, 445), and contained calcitic pedofeatures.
39
40
41
42
43
44
45
46
47
48
49
50
51

52 **Interpretation of micromorphological observations**

53
54
55
56
57
58
59
60

1
2
3
4 The differences in micromorphological characteristics within the Haua Fteah are subtle and
5
6 the features are often undiagnostic when considered in isolation. The observed features were
7
8 therefore interpreted in relation to each other and field observations. Interpretation of structure
9
10 in these layers was hampered by compression by up to 4 m of overlying sediments. In addition,
11
12 the excavation history of the site – excavation, burial, re-excavation – may have altered
13
14 existing, or produced new, redoximorphic features (e.g. dendritic manganese nodules),
15
16 hampering interpretation of whether these features are related to the depositional environment
17
18 of the layers or more ancient redox fluctuations.
19
20
21
22
23
24
25
26

27 The micro-fabrics were divided into three main groups through micromorphological
28
29 observation. The first consists of pale, sandy silt to silt loams containing varying amounts of
30
31 often horizontally-orientated limestone sand and gravel (Figure 6a), probably produced by
32
33 roof-spalling (Farrand, 1975; Laville, 1976; Woodward & Goldberg, 2001; Goldberg &
34
35 Sherwood, 2006). They have largely stipple-specked b-fabrics, implying a lack of mechanical
36
37 processes to orient clays, e.g. shrink-swelling (Kovda & Mermut, 2010), with a micritic
38
39 crystallitic fine component (10–30%) (Figure 6c) interpreted as the inclusion of aeolian
40
41 sediment or spalling of the cave walls. Micritic calcitic crystallitic b-fabrics may also mark
42
43 precipitation of micrite following sediment wetting and drying (Figure 6d) (Durand et al.,
44
45 2010; Goldberg, 1979; Guo & Fedoroff, 1990), as well as the inclusion of ash within the
46
47 sediments (Canti 2003). The nature of the micritic b-fabric in each case was therefore assessed
48
49
50
51
52
53
54
55
56
57
58
59
60

1
2
3
4 via observation of related pedofeatures such as the presence of calcitic wood ash
5
6
7 pseudomorphs (in the case of ash inclusion), or micritic calcitic void hypocoatings formed by
8
9
10 percolation of carbonate-rich water (suggesting post-depositional precipitation). In Context 490
11
12 (Facies 3 Dabban) the formation of micrite and sparite crystals within the groundmass and
13
14
15 pores suggests prolonged dripping onto, and wetting of the cave floor, with extensive
16
17
18 concretion of Micro-Fabrics 2621:2–4. In Micro-fabric 2621:3 (Figure 6d), this calcitic crystal
19
20
21 formation was so extensive that it produced a platy microstructure reminiscent of that formed
22
23
24 by ice crystals in freeze-thaw sediments (e.g. van Vliet-Lanoë, 1998; van Vliet-Lanoë et al.,
25
26
27 1984).

28
29
30 This group of micro-fabrics often contained subtle, sub-millimetre-thick laminations in
31
32
33 the fine material, mirrored in the horizontal orientation of limestone sand and gravel clasts as
34
35
36 well as the presence of horizontal dung lenses (Figure 6e). These features were interpreted as
37
38
39 resulting from punctuated, low-energy, aeolian deposition of fine material, producing
40
41
42 ephemeral surfaces upon which dung was trampled, and limestone clasts fell (Goldberg, 2000).
43
44
45 The dung, which often contains faecal spherulites (Figure 6f), is likely derived through the
46
47
48 activity of herbivores in the cave (Brochier et al., 1992; Canti, 1998, 1999). The wide cave
49
50
51 mouth provides easy access to wild animals seeking shelter. These surfaces may have been
52
53
54 sporadically wetted, producing surface crusts (Goldberg, 2000; Valentin, 1991), or subject to
55
56
57 small-scale washes of clay-rich material from inside the karstic system or through the cave
58
59
60

1
2
3
4 mouth, leaving depositional crusts (Figure 7a) (Bresson & Valentin, 1994; Pagliai & Stoops,
5
6
7 2010; West et al., 1990). Fragments of both sets of crusts were observed, indicating post-
8
9
10 formation trampling or bioturbation. In addition, iron-impregnated aggregates within the
11
12 sediments with a groundmass, internal structure and b-fabric different from the surrounding
13
14 material (Figure 7b) were interpreted as fragments of soil, 'pedorelicts', trampled into or
15
16 around the cave by animals or people (Boschian 1997; Goldberg 1979; Macphail and McAvoy
17
18 2008). Micro-fabrics within this first group of features were therefore interpreted as the
19
20 product of aeolian deposition and reworking on a 'dusty', mainly dry, cave floor, similar to the
21
22 modern cave floor.
23
24
25
26
27
28
29

30 The second main group of deposits examined were silty clay to silty clay loams, generally
31
32 reddish in colour (difficult to assess where slides vary in thickness). Their b-fabrics were
33
34 largely stipple-speckled with some mosaic-speckling (Figure 6b), the latter indicating a limited
35
36 impact of shrink-swell processes, such as drying of a saturated sediment (Cremeens, 2005), and
37
38 were thus interpreted as wet movements of clayey, potentially soil, material. Some contained a
39
40 partially micritic crystallitic b-fabric, usually related to calcitic infillings and hypocoatings and
41
42 therefore interpreted as post-depositional calcite precipitation. Coarse material was often
43
44 arranged chaotically, consistent with a mass depositional event, and the lower boundaries of
45
46 these micro-fabrics are often clear, sharp (Figure 7c) and therefore potentially erosive. On
47
48 occasion, silty clay coatings to voids were present in micro-fabrics directly below these layers
49
50
51
52
53
54
55
56
57
58
59
60

1
2
3
4 (Figure 7d), marking the drainage of water through the profile (French et al., 2009; Kuhn et al.,
5
6
7 2010); their depth restriction suggests that they were linked to short periods of small-scale
8
9
10 illuviation, consistent with clayey water draining from a slurry. The similarity of these micro-
11
12 fabrics to the reddish, clayey local soils led to them being interpreted as resulting from inwash
13
14 of soil material through the cave mouth or elsewhere via the karstic system.
15
16

17
18 Not all observed micro-fabrics fitted perfectly into these two groups. A third group of
19
20 micro-fabrics consisted of silty fine material, coarse limestone sand and partially micritic
21
22 crystallitic b-fabric similar to the 'dusty' micro-fabrics, yet their chaotic arrangement and sharp
23
24 lower boundaries suggest deposition by mass movement, indicating that these layers
25
26 represented reworking of cave-floor material by mass movements. Micro-Fabric 754A:2
27
28 (Context 453) contained a unique combination of features, including distinct horizontal
29
30 laminations and dung lenses, with a mosaic/reticulate b-fabric, dendritic manganese staining
31
32 and partially-dissolved bone (Figure 7e, f). These suggested a layer formed through aeolian
33
34 deposition and reworking that had been subject to prolonged wetting, perhaps marking
35
36 repeated dripping in this area from the cave roof.
37
38
39
40
41
42
43
44
45

46
47 Anthropogenic and biogenic impacts on the sediments were observed
48
49 micromorphologically, with combustion features in Facies 4 and 5 containing layers of finely
50
51 commuted charcoal and ash (Figures 8a, b). Rare charcoal fragments, bone splinters and ash
52
53 lenses were observed throughout, marking a continually reworked 'background' of cultural
54
55
56
57
58
59
60

1
2
3
4 debris. Vesicular silica aggregates observed micromorphologically (Figure 8c) mirrored 'slag'
5
6
7 fragments recovered in the 1950s (McBurney, 1967), formed from the melting of a silica-rich
8
9
10 fuel such as grasses (Canti, 2003; Macphail & Cruise, 2001). Distinct from rounded,
11
12 potentially geogenic clasts, angular splinters of chert were interpreted as knapping micro-
13
14
15 debitage (Figure 8d, Angelucci, 2010). In the large feature from 513/535, ash layers containing
16
17
18 calcitic wood ash pseudomorphs (Figure 8e) indicated the use of wood as fuel (Canti 2003),
19
20
21 and the presence of calcitic hypocoatings (Figure 8f) within these ash layers suggest that the
22
23
24 feature had been subject to post-depositional wetting and weathering, indicating its prolonged
25
26
27 exposure on a surface at the top of Facies 4.
28
29

30 **Bulk Sedimentology**

31 *Particle size analysis*

32
33
34
35
36 The particle size distributions (PSDs) of the non-carbonate <2mm fractions of the Haua
37
38
39 Fteah sediments were largely consistent (Figure 9). Whilst there was variation in mode particle
40
41
42 sizes, the distributions were all bimodal, with a clay peak around 0.17 μ m and a 15.63–44.19 μ m
43
44
45 silt peak. The soil pit distribution (Pit T) shared this bimodal distribution with the Haua Fteah
46
47
48 samples, and, bar a ~353 μ m sand peak, the limestone residue lay within the size ranges of the
49
50
51 Haua Fteah samples.
52

53
54 The consistency in particle size distributions in the non-carbonate fraction indicates that this
55
56
57 fraction of the Haua Fteah sediments did not vary extensively in source or transport mode
58
59
60

1
2
3
4 throughout Facies 5–3. Similarity between the Haua Fteah samples and those from the soil pits
5
6
7 suggest that the local soils, formed on the local limestone, were the primary source of the non-
8
9
10 carbonate sediment, and/or that both shared a common origin. The more marked coarse silt
11
12
13 peak in the particle size distribution in the soil pit, when compared with that from the limestone
14
15
16 residue, indicates another potential input to the soil. The strong sorting in the silt peak may
17
18
19 represent a far-field input of aeolian material, common in Mediterranean soils (Muhs et al.,
20
21
22 2010; Yaalon, 1997). It is possible that the similarity between the limestone residue and the
23
24
25 non-carbonate fraction may be influenced by the dissolution of limestone sand during sample
26
27
28 preparation sample producing non-carbonate residue, yet as mentioned earlier, the very low
29
30
31 non-carbonate content of the limestone (<1%) suggests this addition would not be enough to
32
33
34 skew the PSD. The removal of carbonate from the samples prior to measurement does,
35
36
37 however, raise the possibility that a carbonate-dominated aeolian input directly into cave has
38
39
40 been removed in this analysis.

41 42 *% Loss On Ignition*

43
44
45 All the Facies 5–3 %LOI values from the Haua Fteah were at or below those of the modern
46
47
48 soils (Table 1), suggesting a relative reduction in the organic content of the material after
49
50
51 deposition, or a lower initial organic content to the source material. The values were very
52
53
54 consistent (Standard deviation = 0.5%), rising slowly towards the upper part of the sequence
55
56
57 (Figure 5), with only two small distinct peaks on the North-Facing Profile, one corresponding
58
59
60

1
2
3
4 to combustion features (Contexts 568 and 564) and a context containing frequent dung lenses
5
6
7 (Micro-Fabric 2058:4, Context 536). Such low values and narrow standard deviation means
8
9
10 that it is impossible to infer that these peaks are meaningful. These contexts, which from
11
12 micromorphological observations should have contained significant amounts of organic
13
14 material, had values similar to the modern soils, indicating that in sediments of this age
15
16 (>30,000 years old) %LOI values have, unsurprisingly, decayed to the point at which they are
17
18 no longer meaningful, and little weight should be placed on their interpretation.
19
20
21
22

23 24 *%CaCO₃*

25
26
27 The Haua Fteah samples contained markedly higher %CaCO₃ values than the soil (Table 1),
28
29 indicating the likely addition of carbonate to the sediments if, as appears from the PSDs and
30
31 field observations, that they are dominated by reworked soil material. This addition is likely
32
33 the result of cave wall weathering and post-depositional carbonate precipitation (Goldberg &
34
35 Sherwood, 2006; White, 2007), although it is possible that an aeolian carbonate component
36
37 may also be contributing to the %CaCO₃. Fine clastic carbonate material may also have been
38
39 transported into the shelter in mudflow events. Micromorphological observations of ash, which
40
41 may also have contributed carbonate (Canti 2003) to the sediments are restricted to the thin
42
43 lenses of anthropogenic material in Facies 4 and 5. Broadly, the largest %CaCO₃ peaks
44
45 corresponded to observations of frequent/common coarse sand in the late Facies 5/4 sediments
46
47 (Contexts 520–516, West-Facing Profile; Contexts 537–536, North-Facing Profile, Figure 5),
48
49
50
51
52
53
54
55
56
57
58
59
60

1
2
3
4 yet West-Facing Profile contexts cemented with calcite also corresponded to %CaCO₃ peaks
5
6
7 (Contexts 504–503, 445–442), indicating an equifinality irresolvable without field or
8
9
10 micromorphological data.

11 12 *Magnetic Susceptibility*

13
14
15 Magnetic Susceptibility values varied widely between the soil pits (mean values of 365.45
16
17 and 584.8 m³kg⁻¹), yet these were still largely higher than the cave values (Table 1). Peaks in
18
19 magnetic susceptibility corresponded largely to contexts identified micromorphologically as
20
21 inwashed soil material (e.g. Contexts 508, 498, 493/458–490, Figure 5), yet others were
22
23 associated with 'dusty' cave floor environments (e.g. Contexts 521–523, 563), suggesting that
24
25 another mechanism had raised the values: anthropogenic influence on the sediments, or, less
26
27 likely in caves where pedogenic process are weaker, weathering of the sediments. This
28
29 equifinality meant that the nature of the large jumps in magnetic susceptibility at the top of the
30
31 sampled area, beyond micromorphological sampling, remain ambiguous. Given field
32
33 observations of charcoal in Context 441, these peaks may have been related to burning.
34
35
36
37
38
39
40
41
42
43

44 A negative correlation (-0.588) between %CaCO₃ and magnetic susceptibility reflects the
45
46 major peaks of magnetic susceptibility being largely accompanied by low %CaCO₃ values and
47
48 vice versa. This, and the relatively lower magnetic susceptibility of most of the Haua Fteah
49
50 sediments compared to the soil, may result from the magnetic susceptibility of consistent soil
51
52 material in the cave being 'diluted' by variable amounts of diamagnetic carbonate sand and silt
53
54
55
56
57
58
59
60

1
2
3
4 (Dearing et al., 1985) from the cave walls. Yet correlation of the variables was only moderately
5
6
7 negative, and an R^2 value of 0.35 indicates a broad spread of the data - the impact of the coarse
8
9
10 fraction can, in future be assessed by restricting measurements to the <83um fraction
11
12 (Woodward, 1997a, b). It is also possible that variability in magnetic susceptibility may have
13
14
15 been influenced by source material variation (Ellwood et al., 1997) such as incorporation of
16
17
18 allochthonous carbonate material, or post-deposition burning or weathering (Tite & Mullins,
19
20
21 1971).
22

23 24 **DISCUSSION**

25 26 27 **Methodological Observations: Integrating Field Observations, Micromorphology and** 28 29 30 **Bulk Sedimentology** 31

32
33 The effectiveness of particle size analysis in distinguishing between aeolian and colluvial
34
35
36 deposition at the Haua Fteah appears to have been hampered by the apparent local sediment
37
38
39 source, as the variation between aeolian-dominated and colluvial/inwash deposition observed
40
41
42 in the micromorphology was not identifiable in the particle size distributions. Removal of the
43
44
45 carbonate fraction may have removed a well-sorted aeolian carbonate component, yet it is
46
47
48 unlikely that this component would be solely carbonate - a non-carbonate aeolian element
49
50
51 would be expected to remain identifiable. A poorly-developed lack of a far-field aeolian
52
53
54 signature in the Haua Fteah would be unsurprising given its position on the northern side of the
55
56
57 Gebel Akhdar facing away from the Sahara. The lack of a large area exposed continental shelf
58
59
60

1
2
3
4 during periods of low sea level also limited another past source of aeolian sediment (Lambeck
5
6
7 & Purcell, 2005; GEBCO_14). In addition, the fine material composition observed
8
9
10 micromorphologically is relatively consistent through the sequence (though more clayey within
11
12 the 'mudflow' group); marked variations in fine material source indicating pulses of, for
13
14 example, carbonate beach dune sands might be expected to be visible in the thin sections, but
15
16 are not. The lack of variability seen in the non-carbonate PSDs between layers with quite
17
18 different micromorphologically-observed depositional histories indicates that whilst this data
19
20 can inform on the local source of the non-carbonate fraction, micromorphological observation is
21
22 required to understand the process of deposition.
23
24
25
26
27
28
29

30 Small peaks in bulk %LOI organics appeared to correlate with field and
31
32 micromorphological observations of charred material and dung (Context 536), yet given the
33
34 low values and restricted variation of the dataset, the %LOI values can add little confidence to
35
36 the interpretation of the sequence; the variation may even be influenced more by variation in
37
38 sediment lithology than organic content (Santisteban et al., 2004).
39
40
41
42
43

44 Magnetic susceptibility peaks corresponded frequently with layers interpreted through
45
46 micromorphology and field observations as soil inwash (e.g. Contexts 498 and 508), rather
47
48 than parts of the stratigraphy that had been burnt. An exception may have occurred at the top of
49
50 Facies 3 (Context 441), where charcoal observed in the profiles and an increase in occupation
51
52 material (McBurney, 1967) may account for large magnetic susceptibility peaks. In addition,
53
54
55
56
57
58
59
60

1
2
3
4 not all contexts interpreted micromorphologically as colluvial/wash events were accompanied
5
6
7 by peaks; contexts interpreted micromorphologically as colluvial mass reworking of cave-floor
8
9
10 sediment (e.g. Contexts 497 and 563) lacked high magnetic susceptibility values, confirming
11
12 that magnetic susceptibility may inform on sediment source, but not depositional context.
13
14

15
16 Given the range of processes identified through field observations and micromorphology
17
18 that added carbonate to the sediments, it is largely impossible to interpret the bulk %CaCO₃
19
20 data in isolation. Broad peaks in %CaCO₃ corresponded to increased limestone sand and gravel
21
22 in Facies 4, whilst some of the lowest %CaCO₃ readings corresponded to contexts with high
23
24 magnetic susceptibility interpreted as soil inwash (e.g. Contexts 490 and 498). Yet other
25
26 %CaCO₃ peaks marked contexts containing secondary calcite precipitation (Contexts 503 and
27
28 504) and little limestone sand. No distinct peaks accompanied calcitic ash deposition linked to
29
30 anthropogenic activity in Facies 5, although this may have been due to the small quantities of
31
32 ash involved.
33
34
35
36
37
38
39
40

41
42 It is clear that the bulk sedimentological parameters measured here are subject to issues
43
44 of equifinality. Further clarity of the composition of the bulk sediments through the
45
46 investigation of variation in sedimentological characteristics between different sediment
47
48 fractions (e.g. that of the <63µm fraction following Woodward and Bailey, 2000) or sediment
49
50 sourcing using SEM, XRD or FTIR could, in future, be carried out to understand more fully
51
52 the sources of the material and properties measured. Micromorphological analysis of the Haua
53
54
55
56
57
58
59
60

1
2
3
4 Fteah sediments, however, appears the most robust method of analysis and interpretation of the
5
6
7 final depositional processes that ultimately shaped its stratigraphy.
8

9 10 **Site Formation Processes at the Haua Fteah in Their Mediterranean Context**

11
12 The Haua Fteah sediments show repeated shifts between fine material deposition dominated
13
14 by dry, ‘dusty’ conditions and sporadically wetted surfaces, sometimes with limestone clast
15
16 deposition from the cave walls, and episodic wet, colluvial mass movements. These processes
17
18 are expressed in numerous other Mediterranean Quaternary cave sequences (Frumkin et al.,
19
20 2016; Woodward & Goldberg, 2001), many of which contain archaeological sequences key to
21
22 understanding regional population dynamics and change.
23
24
25
26
27
28
29

30 Mass colluvial deposition of soil material is a common mode of sedimentation noted in
31
32 Mediterranean caves (Albert et al., 1999; Aldeias et al., 2014; Bar-Yosef et al., 1992; Boscian,
33
34 1997; Frumkin et al., 2016; Goder-Goldberger et al., 2012; Goldberg & Bar-Yosef, 1998; Hunt
35
36 et al., 2010, 2011; Woodward & Goldberg, 2001). Whether driven by climate change and/or
37
38 human impact, these movements mark landscape destabilisation (Frumkin et al., 2016;
39
40 Wainwright, 2009), and are largely recorded in caves opening in shallow inclines, or those with
41
42 chimneys such as Konispol, Albania (Schuldenrein, 1998, 2001) and Tabun, Israel (Albert et
43
44 al., 1999). At the Haua Fteah these processes did not dominate the Facies 5–3 sediments, but
45
46 instead occasionally punctuated an otherwise dry cave floor environment. Whilst this reflects
47
48 the susceptibility of the cave to collecting colluvially-deposited sediments, this process was
49
50
51
52
53
54
55
56
57
58
59
60

1
2
3
4 only one of a small number of sedimentation processes that also included aeolian
5
6
7 deposition/reworking and roof spalling.
8

9
10 The aeolian nature of the 'dusty' deposits likewise have Mediterranean parallels. Whilst the
11
12 Haua Fteah lacks wind-deposited beach sand in contrast to caves adjacent to shorelines such as
13
14 Vanguard and Gorham's Caves, Gibraltar (Macphail et al., 2000), fine-grained, aeolian
15
16 sediments were reported from Akrotiri Aetokremnos, Cyprus (Mandel & Simmons, 1997),
17
18 Khef el Ahmmar, Morocco, (Barton et al., 2005), Abri Pataud, France (Farrand, 1975), and
19
20 Klithi, Greece (Woodward 1997a) variously attributed to local sources such as floodplain
21
22 sediments or, as in the Haua Fteah, surrounding hillsides.
23
24
25
26
27
28
29

30 The physical weathering of limestone from cave walls and roofs has long been documented
31
32 in the Mediterranean (Collcutt, 1979; Farrand, 1975; Laville et al., 1980), with
33
34 micromorphological attributes suggesting freeze-thawing as the driver of physical weathering
35
36 at Theopetra, Greece (Karkanas, 1999, 2001), Abric Romani, Spain, and Grotte des Pigeons,
37
38 Taforalt, Morocco (Courty & Vallverdu, 2001). Elsewhere, for example at Ksar Akil, Lebanon
39
40 and Franchthi Cave, Greece (Farrand, 2001b), independent evidence suggests that these sites
41
42 did not experience freezing temperatures and that chemical weathering or wetting/drying
43
44 cycles drove weathering (Goldberg & Sherwood, 2006). Micromorphological structures
45
46 produced by freeze-thawing (e.g. lenticular structures, van Vliet-Lanoë, 1998) were not
47
48 observed in the Haua Fteah, yet its largely dry cave floor may have inhibited their formation.
49
50
51
52
53
54
55
56
57
58
59
60

1
2
3
4 There is often snow on the Gebel Akhdar in winter and current winter temperatures in Shahat,
5
6
7 on the second escarpment, have been recorded as low as 3°C (Libyan National Meteorological
8
9
10 Centre). Regional cooling during glacials and stadials would have further lowered
11
12
13 temperatures, and Pleistocene thermoclastic scree is widespread along the Cyrenaican littoral
14
15
16 (Hey 1963), suggesting that freeze-thaw could have contributed to physical weathering at the
17
18
19 Haua Fteah during certain periods or seasons in addition to ongoing chemical weathering.

20
21 The sediments investigated here show limited carbonate concretion or flowstone
22
23
24 development on the West- and North-Facing Profiles, unlike caves such as Qesem Cave
25
26
27 (Gopher et al., 2010; Karkanas et al., 2007) or Emanuel Cave (Goder-Goldberger et al., 2012),
28
29
30 Israel. The South-Facing Profile sediments, however, and the adjacent northernmost end of the
31
32
33 West-Facing Profile, are heavily cemented, probably because of their proximity to the modern
34
35
36 dripline. The timing of calcite deposition remains unclear, and may considerably post-date the
37
38
39 deposition of the units. This spatial variability suggests that even within a few metres, the
40
41
42 impact of depositional processes can vary, and is dependent on cave morphology as well as
43
44
45 environment.

46
47 The processes that deposited the Haua Fteah sediments are observed in caves across the
48
49
50 Mediterranean. Whilst the dominant processes vary from site to site based on cave morphology
51
52
53 and setting, the variability in sediment energy and rate of deposition between the processes
54
55
56
57
58
59
60

1
2
3
4 highlight the necessity of understanding site formation processes at each and every site in order
5
6
7 to understand the archaeology and palaeoenvironmental sequences within them.
8

9 10 **The Haua Fteah Sediment Sequence and Environmental Drivers**

11
12 Whilst the detailed consideration of the environmental drivers of sedimentation at the Haua
13
14 Fteah with regards to Late Quaternary regional environmental change is beyond the scope of
15
16 this paper, there are general trends that show broad correlation with environmental data (Douka
17
18 et al., 2014; Inglis, 2012). The Facies 5 sediments in the Middle Trench, with a modelled age
19
20 of deposition between 75–64 ka (Douka et al., 2014), correspond to the end of MIS 5a and
21
22 early MIS 4, and consist predominantly of aeolian-deposited fine material, interrupted by
23
24 reworking of cave-floor material in mudflows indicating occasional landscape instability.
25
26
27 There is limited physical weathering of the cave walls shown in occasional limestone clasts,
28
29 yet the sediments are dominated by fine material, indicating that the cave reached the low
30
31 temperatures necessary to accelerate physical weathering of the cave walls through freeze-thaw
32
33 processes. The combustion features appear to have been deposited on dry, unconsolidated
34
35 surfaces, consistent with an environment of aeolian deposition and reworking.
36
37
38
39
40
41
42
43
44
45

46
47 The Facies 4 sediments, with a modelled age of deposition between 68–47 ka,
48
49 (corresponding to MIS 4 and the start of MIS 3), are dominated by limestone gravel and sand,
50
51 the result of increased physical weathering, and reflected in higher %CaCO₃ values.
52
53
54
55
56 Depositional environments remained similar to those of Facies 5, but with increased roof-
57
58
59
60

1
2
3
4 spalling along with fine aeolian deposition and reworking, likely the result of MIS 4 driven
5
6 cooling that activated freeze-thaw weathering. Sporadic wetting of the largely dry sediments
7
8 continued, but more numerous mudflows into the cave (compared with Facies 5), marked
9
10 increased frequency of landscape instability. At the top of the facies, extended exposure and
11
12 weathering of a large burning event supports a sediment hiatus that is also suggested by the
13
14 chronology (Douka et al., 2014; Inglis, 2012).
15
16
17
18
19

20
21 Facies 3 sediments, with a modelled age of between 48–34 ka (falling within equivalent
22
23 MIS 3), were marked by smaller quantities of carbonate gravel and sand indicating an overall
24
25 reduction in physical weathering, and therefore potentially warmer temperatures than in MIS 4.
26
27 Limestone clast deposition in contexts towards the top of the facies indicate shorter-lived drops
28
29 in temperatures. As in Facies 4, the deposition of fine material varied between ‘dusty’
30
31 environments and mudflow deposition. The red, clayey, mudflow sediments with high
32
33 magnetic susceptibility towards the top of the facies, accompanying the layers containing
34
35 limestone clasts, suggest the increasingly frequent transport into the cave of well-developed
36
37 soils or subsoil horizons from the landscape during periods of landscape instability, potentially
38
39 driven by increasingly cool periods along a downward temperature trend towards the gravel-
40
41 dominated MIS 2.
42
43
44
45
46
47
48
49
50
51

52 **Site Formation Processes and Assessment of the Haa Fteah Stratigraphy**

53
54
55
56
57
58
59
60

1
2
3
4 The analysis of the Haua Fteah sediments has identified two predominant modes of
5
6
7 deposition, fine aeolian deposition/reworking, and mudflows of external or internal material.
8
9
10 These represent very different taphonomic pathways, and major interpretative implications, for
11
12 the archaeological and palaeoenvironmental material preserved within them, with significant
13
14 implications for similar 'cornerstone' archaeological sequences established from cave
15
16 stratigraphies.
17
18
19

20
21 In terms of the impact on the interpretation of palaeoenvironmental proxies, 'dusty'
22
23 deposition, with its continual small-scale surface reworking of fine material on a dry cave
24
25 floor, would, with its slow net rate of deposition, allow sediments to blow into and around the
26
27 cave over an extended period of time, mixing with material already deposited in the cave.
28
29
30 These layers likely contain assemblages of environmental proxies that have been subject to
31
32 'time averaging'. For example, rapid vegetation change may not have been recorded if the
33
34 mode of deposition in the cave remained constant; new proxy assemblages would be mixed
35
36 with those already within the cave, creating assemblages that did not bear direct relation to the
37
38 outside environment, and which masked shorter-term environmental fluctuations. In contrast,
39
40 the rapid deposition of the mudflow events would avoid this degree of time averaging, but may
41
42 also have transported and re-deposited pollen or phytoliths or other material inherited from
43
44 soils or sediments already existing in the landscape (e.g. Hunt et al., 2015). Abrupt changes
45
46 identified in palaeoenvironmental indicators as recorded in the CPP sample columns may
47
48
49
50
51
52
53
54
55
56
57
58
59
60

1
2
3
4 therefore be more due to changes in taphonomic pathway than environment, whilst periods of
5
6 consistency may mask a more complex picture, highlighting the need to ground
7
8 palaeoenvironmental interpretation within the detailed stratigraphic framework that this study
9
10 has provided.
11
12
13

14
15 The varying rates and modes of deposition would have had similar effects on the
16
17 archaeological assemblages within them. Low energy, aeolian depositional environments and
18
19 their slow net rate of aggradation may have meant that artefacts were exposed on, or very near
20
21 to, the surface for variable periods of time, during which they may have been trampled or
22
23 disturbed by animals and/or humans. In addition, during their exposure, artefacts may have
24
25 been moved, recycled or completely removed by humans (Bailey, 2007; Vaquero et al., 2012).
26
27 Material on these slowly aggrading surfaces may have been deposited in a single episode of
28
29 activity, or through multiple episodes during low net sedimentation, thus forming palimpsests
30
31 of increasing time depth (Bailey & Galanidou, 2009; Stern, 2008). These 'dusty' layers
32
33 therefore have relatively low chronological and behavioural resolution, even if the artefacts
34
35 have not been moved by the sedimentation processes or later activity, and they may even
36
37 contain artefacts from different cultural groups, blurring cultural transitions that were in fact
38
39 quite abrupt. In contrast, the mudflow layers were deposited in single, or a series of very
40
41 temporally constrained depositional, events (e.g. days), potentially burying artefacts soon after
42
43 deposition, but also potentially producing archaeologically 'sterile' layers that could appear to
44
45
46
47
48
49
50
51
52
53
54
55
56
57
58
59
60

1
2
3
4 represent occupation hiatuses, but may only mark a day or less of rapid deposition. Such
5
6
7 movements may rework archaeological material from elsewhere in the cave, or from the
8
9
10 surface of the landscape outside the cave. Again, the taphonomic impact of the sediments must
11
12
13 be borne in mind when interpreting the changing densities of archaeology throughout the
14
15
16 sequence, and their behavioural implications.

17
18 These changing processes, and their changing depositional energies, are crucial to
19
20
21 understanding the stratigraphic integrity of the MSA/LSA 'transition' in Layer XXV of the
22
23
24 Haia Fteah. McBurney identified reworking, or population turnover, as a potential reason for
25
26
27 the apparent interstratification of Levallois-Mousterian and Dabban material in Layer XXV.
28
29
30 The identification of mudflow deposits within Layer XXV provides support to the reworking
31
32
33 hypothesis, yet Layer XXV also contains layers built up through dusty/aeolian sedimentation –
34
35
36 if the different artefact assemblages were contained within these layers, they may not have
37
38
39 been reworked or mixed by mudflows. Correlation of the McBurney archaeological archive
40
41
42 with specific CPP contexts, with the degree of resolution required to resolve the question of the
43
44
45 integrity of the transitional layers, poses a major challenge for the CPP investigations. The
46
47
48 renewed investigations provide the increased stratigraphic resolution which could address these
49
50
51 issues, yet the Facies 3 layers in the new excavations (Trench M) have yielded a very low
52
53
54 number of artefacts (Farr et al., 2014). We are left with, on the one hand, a poorly
55
56
57 stratigraphically constrained archive with enough artefacts – though one still low in number in
58
59
60

1
2
3
4 these levels (McBurney 1967) – to identify shifts in technology, and on the other, a well
5
6 stratigraphically well-constrained record which contains few artefacts that are unable to
7
8 pinpoint robustly where in the stratigraphy this transition occurred. An enhanced understanding
9
10 of the taphonomy of the key MSA/LSA layers, and its implications for the archaeological
11
12 record within them, may therefore remain challenging.
13
14
15
16

17 18 **CONCLUSION**

19
20 Detailed geoarchaeological analysis of the Haua Fteah sediments integrating field
21
22 observations, micromorphology and bulk sediment analyses has demonstrated the modes of
23
24 formation of the sediments comprising the late MSA–early LSA layers of one of the key North
25
26 African cultural sequences. Sedimentation throughout this period, characterised as Facies 5–3,
27
28 was dominated by low-energy, slow net aeolian sedimentation and reworking, interrupted by
29
30 mass movements of material from outside or inside the cave. These changing depositional
31
32 environments have important implications for understanding the archaeological sequence and
33
34 the cultural transitions within it, because the layers represent different taphonomic histories.
35
36 Whilst the reconstruction of the environmental drivers behind the changing sedimentation
37
38 processes at the Haua Fteah require more discussion than is possible here, this work
39
40 demonstrates that the environmental conditions in which caves were inhabited had profound
41
42 implications for the nature of the record that is preserved of these occupations.
43
44
45
46
47
48
49
50
51
52
53
54
55
56
57
58
59
60

1
2
3
4 The varying site formation processes observed through the MSA and LSA levels, the
5
6
7 limited archaeological resolution of the sequence excavated by McBurney, and the low
8
9
10 numbers of stratigraphically-constrained artefacts from the new excavations, mean that a
11
12
13 higher-resolution assessment of the MSA/LSA transition and its palaeoenvironmental
14
15
16 conditions through the Haua Fteah sequence remains difficult. Full analysis of the findings
17
18
19 from the new excavations will improve the stratigraphic understanding of the newly-recovered
20
21
22 artefacts, their sedimentological context, and the extent to which reworking may have affected
23
24
25 the observed sequence, though it remains possible that, given issues of sediment redeposition,
26
27
28 the Haua Fteah sequence may not preserve a 'high-resolution' record of the nature, conditions
29
30
31 and timing of some of the key cultural transitions that took place within the ca. 140,000-year
32
33
34 human frequentation of the site. Most importantly, the sediment formation processes
35
36
37 recognised in the Haua Fteah, and the issues of archaeological interpretation raised by these
38
39
40 findings, are consistent with those of many other human occupation caves in the Mediterranean
41
42
43 region (and indeed beyond), highlighting the necessity to employ a battery of
44
45
46 geoarchaeological analyses to establish the limitations and potential of the archaeological and
47
48
49 palaeoenvironmental records contained within them, and the regional and global chronologies
50
51
52 they underpin. The complex relationship between changing sedimentation processes at the
53
54
55 Haua Fteah and the iconic cultural record in it established by the 1950s excavations is a
56
57
58 powerful case study demonstrating that the environmental conditions in which caves were
59
60

1
2
3
4 inhabited has profound implications for the nature of the human occupation records that are
5
6
7 preserved in them, and for the wider cultural interpretations that are built on such records.
8

9 10 **ACKNOWLEDGEMENTS**

11
12 RHI's PhD research was funded by an Arts and Humanities Research Council Doctoral
13
14 Award and Magdalene College, Cambridge. We also thank in particular the Department of
15
16 Antiquities of Libya for its permission to undertake the new excavations at the Haua Fteah, and
17
18 their logistical support for the fieldwork. The project was initially termed the Cyrenaican
19
20 Prehistory Project, with the excavation permit arranged by and funding provided by the Society
21
22 for Libyan Studies, whose support is gratefully acknowledged. From 2009, it has also been
23
24 termed the TRANS-NAP project from the acronym of the European Research Council grant to
25
26 GB (Advanced Investigator Grant 230421: "Cultural Transformations and Environmental
27
28 Transitions in North African Prehistory"), which has provided the major funding for the project
29
30 that is also gratefully acknowledged. The support of the Natural Environment Research
31
32 Council's Radiocarbon Facility is also acknowledged. The authors thank Geoff Bailey for his
33
34 valuable comments on a draft of this manuscript, and the three anonymous reviewers for their
35
36 helpful comments.
37
38
39
40
41
42
43
44
45
46
47
48
49
50
51
52
53
54
55
56
57
58
59
60

REFERENCES

- 1
2
3
4
5
6 Albert, R.M., Lavi, O., Estroff, L., Weiner, S., Tsatskin, A., Ronen, A., Lev-Yadun, S. (1999).
7 Mode of occupation of Tabun Cave, Mt Carmel, Israel during the Mousterian period: A
8 study of the sediments and phytoliths. *Journal of Archaeological Science*, 26, 1249–
9 1260.
- 10
11 Aldeias, V., Goldberg, P., Dibble, H.L., & El-Hajraoui, M. (2014). Deciphering site formation
12 processes through soil micromorphology at Contrebandiers Cave, Morocco. *Journal of*
13 *Human Evolution*, 69, 8–30.
- 14
15
16 Ambrose, S.H. (1998). Late Pleistocene human population bottlenecks, volcanic winter, and
17 differentiation of modern humans. *Journal of Human Evolution*, 34, 623–651.
- 18
19 Ambrose, S.H. (2003). Did the super-eruption of Toba cause a human population bottleneck?
20 Reply to Gathorne-Hardy and Harcourt-Smith. *Journal of Human Evolution*, 45, 231–
21 237.
- 22
23 Angelucci, D.E. (2010). The recognition and description of knapped lithic artifacts in thin
24 section. *Geoarchaeology*, 25 (2), 220–232.
- 25
26 Bailey, G.N. (2007). Time perspectives, palimpsests and the archaeology of time. *Journal of*
27 *Anthropological Archaeology*, 26, 198–223.
- 28
29 Bailey, G.N., & Flemming, N. (2008). Archaeology of the continental shelf: Marine resources,
30 submerged landscapes and underwater archaeology. *Quaternary Science Reviews*,
31 27(23–24), 2153–2165.
- 32
33 Bailey, G.N., & Galanidou, N. (2009). Caves, palimpsests and dwelling spaces: examples from
34 the Upper Palaeolithic of south-east Europe. *World Archaeology*, 41(2), 215–241.
- 35
36 Bailey G.N., Woodward, J.C. (1997) The Klithi deposits: sedimentology, stratigraphy and
37 chronology. In: Bailey G.N. (ed) *Klithi: Palaeolithic Settlement and Quaternary*
38 *Landscapes in Northwest Greece*, vol 1. (pp. 61–94) Cambridge: McDonald Institute
39 for Archaeological Research.
- 40
41
42 Bar-Yosef, O., Vandermeersch B, Arensburg, B., Belfer-Cohen, A., Goldberg, P., Laville, H.,
43 Meignen, L., Rak, Y., Speth, J.D., Tchernov, E., Tillier, A.-M., & Weiner, S. (1992).
44 The excavations in Kebara Cave, Mt. Carmel. *Current Anthropology*, 33(5), 497–550.
- 45
46 Barham, L., & Mitchell, P. (2008). *The First Africans*. Cambridge: Cambridge University
47 Press.
- 48
49 Barker, G., Hunt, C.O., Reynolds, T., Brooks, I., & el-Rishi, H. (2007). The Haua Fteah,
50 Cyrenaica (Northeast Libya): renewed investigations of the cave and its landscape,
51 2007. *Libyan Studies*, 38, 93–114.
- 52
53
54 Barker, G., Basell, L., Brooks, I., Cartwright, C., Cole, F., Davison, J., Farr, L., Grün, R.,
55 Hamilton, R., Hunt, C., Inglis, R.H., Jacobs, Z., Legge, T., Leitch, V., Morales, J.,
56 Morley, I., Morley, M., Pawley, S., Pryor, A., Roberts, R., Reynolds, T., el-Rishi, H.,
57
58
59
60

- 1
2
3 Simpson, D., Twati, M., & van der Veen, M. (2008). The Cyrenaican Prehistory Project
4 2008: the second season of investigations of the Haua Fteah cave and its landscape, and
5 further results from the initial (2007) fieldwork. *Libyan Studies*, 39, 175–221.
- 6
7
8 Barker, G., Antoniadou, A., Barton, H., Brooks, I., Candy, I., Drake, N.A., Farr, L., Hunt, C.,
9 Ibrahim, A.A., Inglis, R., Jones, S., Morales, J., Morley, I., Mutri, G., Rabett, R.,
10 Reynolds, T., Simpson, D., Twati, M., & White, K. (2009). The Cyrenaican Prehistory
11 Project 2009: the third season of investigations of the Haua Fteah cave and its
12 landscape, and further results from the 2007–2008 fieldwork. *Libyan Studies*, 40, 55–
13 94.
- 14
15
16 Barker, G., Antoniadou, A., Armitage, S., Brooks, I., Candy, I., Connell, K., Douka, K., Drake,
17 N., Farr, L., Hill, E., Hunt, C., Inglis, R., Jones, S., Lane, C., Lucarini, G., Meneeley, J.,
18 Morales, J., Mutri, G., Prendergast, A., Rabett, R., Reade, H., Reynolds, T., Russell, N.,
19 Simpson, D., Smith, B., Stimpson, C., Twati, M., & White, K. (2010). The Cyrenaican
20 Prehistory Project 2010: the fourth season of investigations of the Haua Fteah cave and
21 its landscape, and further results from the 2007–2009 fieldwork. *Libyan Studies*, 41,
22 63–88.
- 23
24
25
26 Barker, G., Bennett, P., Farr, L., Hill, E., Hunt, C., Lucarini, G., Morales, J., Mutri, G.,
27 Prendergast, A., Pryor, A., Rabett, R., Reynolds, T., Spry-Marques, P., & Twati, M.
28 (2012). The Cyrenaican Prehistory Project 2012: The fifth season of investigations at
29 the Haua Fteah cave. *Libyan Studies*, 43, 115–136.
- 30
31
32 Barton, R.N.E., Bouzouggar, A., Collcutt, S., Gale, R., Higham, T., Humphrey, L.T., Parfitt,
33 S., Rhodes, E., Stringer, C., & Malek, F. (2005). The Late Upper Palaeolithic
34 occupation of the Moroccan Northwest Maghreb during the Last Glacial Maximum.
35 *African Archaeological Review*, 22(2), 77–100.
- 36
37
38 Barton, R.N.E., Bouzouggar A., Hogue J., Lee S., Collcutt S.N., & Ditchfield P. (2013).
39 Origins of the Iberomaurusian in NW Africa: New AMS radiocarbon dating of the
40 Middle and Later Stone Age deposits at Taforalt Cave, Morocco. *Journal of Human*
41 *Evolution*, 65, 266–281.
- 42
43
44 Barton, R.N.E., Lane, C.S., Albert, P.G., White, D., Collcutt, S.N., Bouzouggar, A., Ditchfield,
45 P., Farr, L., Oh, A., Ottolini, L., Smith, V.C., Van Peer, P., & Kindermann, K. (2015).
46 The role of cryptotephra in refining the chronology of Late Pleistocene human
47 evolution and cultural change in North Africa. *Quaternary Science Reviews*, 118, 151–
48 169.
- 49
50
51 Barton, R.N.E., Bouzouggar, A., Collcutt, S.N., Carrión Marco, Y., Clark-Balzan, L.,
52 Debenham, N.C., Morales, J. (2016). Reconsidering the MSA to LSA transition at
53 Taforalt Cave (Morocco) in the light of new multi-proxy dating evidence. *Quaternary*
54 *International*, 413, 36–49
- 55
56
57
58
59
60

- 1
2
3 Benazzi, S., Douka, K., Fornai, C., Bauer, C.C., Kullmer, O., Svoboda, J., Pap I., Mallegni, F.,
4 Bayle, P., Coquerelle, M., Condemi, S., Ronchitelli, A., Harvati, K., & Weber, G.W.
5 (2011). Early dispersal of modern humans in Europe and implications for Neanderthal
6 behaviour. *Nature*, 479(7374), 525–528.
7
8
9 Boscian, G. (1997). Sedimentology and Soil Micromorphology of the Late Pleistocene and
10 Early Holocene Deposits of Grotta dell'Edera (Trieste Karst, NE Italy).
11 *Geoarchaeology*, 12(3), 227–249.
12
13 Bresson, L.M., & Valentin, C. (1994). Soil surface crust formation: contribution of
14 micromorphology. In A.J. Ringrose-Voase & G.S. Humphreys (Eds.), *Soil*
15 *Micromorphology: Studies in Management and Genesis. Proceedings of the IX*
16 *International Working Meeting on Soil Micromorphology, Townsville, Australia, July*
17 *1992*. (pp. 737–757). Amsterdam: Elsevier.
18
19
20 Brochier, J. E., Villa, P., & Giacomarra, M. (1992). Shepherds and Sediments: geo-
21 ethnoarchaeology of pastoral sites. *Journal of Anthropological Archaeology*, 11, 42–
22 102.
23
24
25 Bullock, P., Fédoroff, N., Jongerius, A., Stoops, G., & Tursina, T. (1985). *Handbook for Soil*
26 *Thin Section Description*. Wolverhampton: Waine Research Publications.
27
28 Butzer, K.W. (1971). *Environment and Archeology: An Ecological Approach to Prehistory*.
29 London: Meuthen.
30
31 Cancellieri, E., Cremaschi, M., Zerboni, A., & di Lernia, S. (2016). Climate, environment and
32 population dynamics in Pleistocene Sahara. In S.C. Jones & B.A. Stewart (Eds.), *Africa*
33 *from MIS 6–2: Population Dynamics and Paleoenvironments* (pp. 123–145).
34 Dordrecht: Springer.
35
36
37 Canti, M. G. (1998) The micromorphological identification of faecal spherulites from
38 archaeological and modern materials. *Journal of Archaeological Science*, 25, 435–44.
39
40 Canti, M. G. (1999) The production and preservation of faecal spherulites: animals,
41 environment and taphonomy. *Journal of Archaeological Science*, 26, 251–58.
42
43 Canti, M. G. (2003) Aspects of the chemical and microscopic characteristics of plant ashes
44 found in archaeological soils. *Catena*, 54, 339–61.
45
46 Campy, M., & Chaline, J. (1993). Missing records and depositional breaks in French Late
47 Pleistocene cave sediments. *Quaternary Research*, 40, 318–331.
48
49 Canti, M.G. (2003). Aspects of the chemical and microscopic characteristics of plant ashes
50 found in archaeological soils. *Catena*, 54, 339–361.
51
52 Collcutt, S.N. (1979). The analysis of Quaternary cave sediments. *World Archaeology*, 10(3),
53 290–301.
54
55 Coudé-Gaussen, G., & Rognon, P. (1993). Contrasting origin and character of Pleistocene and
56 Holocene dust falls on the Canary Islands and southern Morocco: genetic and climatic
57
58
59
60

- 1
2
3 significance. In K. Pye (Ed.), *The Dynamics and Environmental Context of Aeolian*
4 *Sedimentary Systems* (pp. 277–291). London: The Geological Society.
- 5
6 Courty, M.-A., & Vallverdu, J. (2001). The microstratigraphic record of abrupt climate
7 changes in cave sediments of the Western Mediterranean. *Geoarchaeology*, 16(5), 467–
8 500.
- 9
10 Courty, M.-A., Goldberg, P., & Macphail, R.I. (1989). *Soils and Micromorphology in*
11 *Archaeology*. Cambridge: Cambridge University Press.
- 12
13 Cremeens, D.L. (2005). Micromorphology of Cotiga Mound, West Virginia. *Geoarchaeology*,
14 20(6), 581–597.
- 15
16 Dearing, J.A., Maher, B.A., & Oldfield, F. (1985). Geomorphological linkages between soils
17 and sediments: the role of magnetic measurements. In K.S. Richards, R.R. Arnett & S.
18 Ellis (Eds.), *Geomorphology and Soils* (pp. 245–267). London: George Allen & Unwin.
- 19
20 Di Vito, M.A., Sulpizio, R., Zanchetta, G., & D’Orazio, M. (2008). The late Pleistocene
21 pyroclastic deposits of the Campanian Plain: new insights into the explosive activity of
22 Neapolitan volcanoes. *Journal of Volcanology and Geothermal Research*, 177, 19–48.
- 23
24 Douka, K., Grün, R., Jacobs, Z., Lane, C., Farr, L., Hunt, C., Inglis, R.H., Reynolds, T., Albert,
25 P., Aubert, M., Cullen, V., Hill, E., Kinsley, L., Roberts, R.G., Tomlinson, E.L., Wulf,
26 S., & Barker, G. (2014). Redating the Haua Fteah cave (Cyrenaica, northeast Libya)
27 and its implications for North African prehistory. *Journal of Human Evolution*, 66, 39–
28 63.
- 29
30 Drake, N., & Breeze, P. (2016). Climate Change and Modern Human Occupation of the Sahara
31 from MIS 6–2. In S.C. Jones & B.A. Stewart (Eds.), *Africa from MIS 6–2: Population*
32 *Dynamics and Palaeoenvironments* (pp. 103–122). Amsterdam: Springer Verlag.
- 33
34 Drake, N.A., Breeze, P., & Parker, A. (2013). Palaeoclimate in the Saharan and Arabian
35 Deserts during the Middle Palaeolithic and the potential for hominin dispersals.
36 *Quaternary International*, 300, 48–61.
- 37
38 Durand, N., Monger, H.C., & Canti, M.G. (2010). Calcium carbonate features. In G. Stoops, V.
39 Marcelino & F. Mees (Eds.), *Interpretation of Micromorphological Features of Soils*
40 *and Regoliths* (pp. 149–194). Amsterdam: Elsevier.
- 41
42 Ellis, S., & Mellor, A. (1995). *Soils and Environment*. London: Routledge.
- 43
44 Ellwood, B.B., Harrold, F.B., L, B.S., Thacker, P., Otte, M., Bonjean, D., Long, G.J., Shahin,
45 A.M., Hermann, R.P., & Grandjean, F. (2004). Magnetic susceptibility applied as an
46 age–depth–climate relative dating technique using sediments from Scladina Cave, a
47 Late Pleistocene cave site in Belgium. *Journal of Archaeological Science*, 31, 283–293.
- 48
49 Ellwood, B.B., Petruso, K.M., Harrold, F.B., & Schuldenrein, J. (1997). High-resolution
50 paleoclimatic trends for the Holocene identified using magnetic susceptibility data from
51 archaeological excavations in caves. *Journal of Archaeological Science*, 24, 569–573.
- 52
53
54
55
56
57
58
59
60

- 1
2
3 Farr, L., Lane, R., Abdulazeez, F., Bennett, P., Holman, J., Marasi, A., Prendergast, A., Al-
4 Zweyi, M., & Barker, G. (2014). The Cyrenaican Prehistory Project 2013: the seventh
5 season of excavations in the Haa Fteah cave. *Libyan Studies*, 45, 163–173.
- 6
7 Farrand, W.R. (1975). Sediment analysis of a prehistoric rockshelter: the Abri Pataud.
8 *Quaternary Research*, 5, 1–26.
- 9
10 Farrand, W.R. (2001). Archaeological sediments in rockshelters and caves. In J.K. Stein (Ed.),
11 *Sediments in Archaeological Context* (pp. 29–66). Salt Lake City: University of Utah
12 Press.
- 13
14 Foley, R.A., & Lahr, M.M. (1997). Mode 3 technologies and the evolution of modern humans.
15 *Cambridge Archaeological Journal*, 7(1), 3–36.
- 16
17 Folk, R.L. (1966). A review of grain-size parameters. *Sedimentology*, 6, 73–93.
- 18
19 French, C.A.I., Sulas, F., & Madella, M. (2009). New geoarchaeological investigations of the
20 valley systems in the Aksum area of northern Ethiopia. *Catena*, 78, 218–233.
- 21
22 Frumkin, A., Langford, B., Marder, O., & Ullman, M. (2016). Paleolithic caves and hillslope
23 processes in south-western Samaria, Israel: Environmental and archaeological
24 implications. *Quaternary International*, 398, 246–258.
- 25
26 Gale, S., & Hoare, P.G. (1991). *Quaternary Sediments: Petrographic Methods for the Study of*
27 *Unlithified Rocks*. London: Bellhaven.
- 28
29 Garcea, E.A.A. (2004). Crossing deserts and avoiding seas: Aterian North African-European
30 relations. *Journal of Anthropological Research*, 60, 27–53.
- 31
32 Garcea, E. E. A. (2010). The Lower and Upper Later Stone Age of North Africa. In Garcea
33 E.A.A. (Ed.) *South-Eastern Mediterranean Peoples Between 130,000 and 10,000 Years*
34 *Ago* (pp. 66–88). Oxford: Oxbow.
- 35
36 Garcea, E.A.A. (2012). Successes and failures of human dispersals from North Africa.
37 *Quaternary International*, 270, 110–128.
- 38
39 Garcea, E.E.A. (2016). Dispersals out of Africa and back to Africa: Modern origins in North
40 Africa. *Quaternary International*, 408, 79–89.
- 41
42 Garcea E.A.A., Giraudi C. (2006) Late Quaternary human settlement patterning in the Jebel
43 Gharbi. *Journal of Human Evolution*, 51(4), 411–421
- 44
45 GEBCO_14 (2014). *General Bathymetric Chart of the Oceans 30-Arc Second Grid*. British
46 Oceanographic Data Centre.
- 47
48 Geyh, M.A., & Thiedig, F. (2008). The Middle Pleistocene Al Mahrúqah formation in the
49 Murzuq Basin, northern Sahara, Libya: evidence for orbitally forced humid episodes
50 during the last 500,000 years. *Palaeogeography, Palaeoclimatology, Palaeoecology*,
51 257(1), 1–21.
- 52
53 Giraudi, C. (2005). Eolian sand in peridesert northwestern Libya and implications for Late
54 Pleistocene and Holocene Sahara expansions. *Palaeogeography, Palaeoclimatology,*
55 *Palaeoecology*, 218, 161–173.
- 56
57
58
59
60

- 1
2
3 Goder-Goldeber, M., Edwards, R.L., Marder, O., Peleg, Y., Yeshurun, R., Frumkin, A., &
4 Grigson, C. (2012). Emanuel Cave (Israel): The Site and its Bearing on Early Middle
5 Paleolithic Technological Variability. *Paléorient*, 38(1), 203–225.
- 6
7 Goldberg, P. (1979). Micromorphology of Pech-de-l'Azé II Sediments. *Journal of*
8 *Archaeological Science*, 6, 17–47.
- 9
10 Goldberg, P. (2000). Micromorphology and site formation at Die Kelders Cave I, South Africa.
11 *Journal of Human Evolution*, 38, 43–90.
- 12
13 Goldberg, P., & Bar-Yosef, O. (1998). Site formation processes in Kebara and Hayonim caves
14 and their significance in Levantine prehistoric caves. In T. Akazawa, K. Aoki & B.-Y.
15 O (Eds.), *Neanderthals and Modern Humans in Western Asia* (pp. 107–126). New
16 York: Plenum Press.
- 17
18 Goldberg, P., & Sherwood, S.C. (2006). Deciphering human prehistory through the
19 geoarchaeological study of cave sediments. *Evolutionary Anthropology*, 15, 20–36.
- 20
21 Gopher, A., Ayalon, A., Bar-Matthews, M., Barkai, R., Frumkin, A., Karkanas, P., Shahack-
22 Gross, R. (2010) The chronology of the late Lower Paleolithic in the Levant based on
23 U-Th ages of speleothems from Qesem Cave, Israel. *Quaternary Geochronology*, 5,
24 644–656
- 25
26 Guo, Z.T., & Fedoroff, N. (1990). Genesis of calcium carbonate in loess and in palaeosols in
27 central China. In L.A. Douglas (Ed.), *Soil Micromorphology: A Basic and Applied*
28 *Science. Proceedings of the VIIIth International Working Meeting on Soil*
29 *Micromorphology, San Antonio, Texas, July 1988* (pp. 355–359). Amsterdam: Elsevier.
- 30
31 Harris, E. (1989). *Principles of Archaeological Stratigraphy* (2nd ed.). London: Academic
32 Press.
- 33
34 Hey, R.W. (1963). Pleistocene screes in Cyrenaica. *Eiszeitalter und Gegenwart*, 14, 77–84.
- 35
36 Higham, T.F.G., Compton, T., Stringer, C.B., Jacobi, R., Shapiro, B., Trinkaus, E., Chandler,
37 B., Gröning, F., Collins, C., Hillson, S., O'Higgins, P., FitzGerald, C., Fagan, M., &
38 Taçon, P.S.C. (2011). The earliest evidence for anatomically modern humans in
39 northwestern Europe. *Nature*, 479, 521–524.
- 40
41 Hoffmann, D.L., Rogerson, M., Spötl, C., Leutscher, M., Vance, D., Osborne, A.H., Fello,
42 N.M., & Moseley, G.E. (2016). Timing and causes of North African wet phases during
43 the last glacial period and implications for modern human migration. *Scientific Reports*
44 6, 36367.
- 45
46 Hublin, J.J. (1992). Recent human evolution in northwestern Africa. *Philosophical*
47 *Transactions: Biological Sciences* 377(1280) 185–91.
- 48
49 Hublin, J.J. (2001). Northwestern African Middle Pleistocene hominids and their bearing on
50 the emergence of *Homo sapiens*. In L. Barham & K. Robson-Brown (Eds).. *Human*
51 *Roots: Africa and Asia in the Middle Pleistocene* (pp 99–122). Bristol: Western
52 Academic & Specialist Press.
- 53
54
55
56
57
58
59
60

- 1
2
3 Hunt, C., Davison, J., Inglis, R., Farr, L., Reynolds, T., Simpson, D., el-Rishi, H., &
4 Barker, G. (2010). Site formation processes in caves: The Holocene sediments of the Haua
5 Fteah, Cyrenaica, Libya. *Journal of Archaeological Science*, 37, 1600–1611.
- 6
7 Hunt, C., Brooks, I., Meneeley, J., Brown, D., Buzaian, A., & Barker, G. (2011). The
8
9 Cyrenaican Prehistory Project 2011: Late-Holocene environments and human activity
10 from a cave fill in Cyrenaica, Libya. *Libyan Studies*, 42, 77–88.
- 11
12 Hunt, C.O., Gilbertson, D.D., Hill, E.A., & Simpson, D. (2015). Sedimentation, re-
13 sedimentation and chronologies in archaeologically-important caves: problems and
14 prospects. *Journal of Archaeological Science*, 56, 109–116.
- 15
16 Inglis, R.H. (2012). *Human Occupation and Changing Environments During the Middle to*
17 *Later Stone Ages: Soil Micromorphology at the Haua Fteah, Libya*. Unpublished
18 doctoral dissertation, University of Cambridge.
- 19
20
21 Jacobs, Z., Li, B., Farr, L., Hill, E., Hunt, C.O., Jones, S., Rabett, R., Reynolds, T., Roberts,
22 R.G., Simpson, D., & Barker, G., (2017). The chronostratigraphy of the Haua Fteah
23 cave (Cyrenaica, northeast Libya) Optical dating of early human occupation during
24 Marine Isotope Stages 4, 5 and 6. *Journal of Human Evolution*, 105, 69–88.
- 25
26 Jones, S., Antoniadou, A., Barton, H., Drake, N., Farr, L., Hunt, C., Inglis, R., Reynolds, T.,
27 White, K., & Barker, G., (2016). Patterns of hominin occupation and cultural diversity
28 across the Gebel Akhdar of Northern Libya over the last ~200 ka. In S. Jones, & B.
29 Stewart. (Eds.) *Africa from MIS 6–2: Population Dynamics and Palaeoenvironments*,
30 Springer (pp. 77–99). Dordrecht: Springer.
- 31
32
33 Jones, S.C. & Stewart, B.A. (Eds.) (2016). *Africa from MIS 6–2: Population Dynamics and*
34 *Palaeoenvironments*. Dordrecht: Springer.
- 35
36
37 Karkanas, P. (1999). Lithostratigraphy and micromorphology of Theopetra Cave deposits
38 Thessaly, Greece: Some Preliminary Results. *British School at Athens Studies*, 3, 240–
39 251.
- 40
41 Karkanas, P. (2001). Site formation processes in Theopetra Cave: a record of climatic change
42 during the Late Pleistocene and Early Holocene in Thessaly, Greece. *Geoarchaeology*,
43 16(4), 373–399.
- 44
45 Karkanas, P., & Goldberg, P. (2010). Site formation processes at Pinnacle Point Cave 13B
46 (Mossel Bay, Western Cape Province, South Africa): resolving stratigraphic and
47 depositional complexities with micromorphology. *Journal of Human Evolution*, 59(3–
48 4), 256–273.
- 49
50
51 Karkanas, P., Shahack-Gross, R., Ayalon, A., Bar-Matthews, M., Barkai, R., Frumkin, A.,
52 Gopher, A., & Stiner, M. C. (2007) Evidence for habitual use of fire at the end of the
53 Lower Paleolithic: Site-formation processes at Qesem Cave, Israel. *Journal of Human*
54 *Evolution*, 53, 197–212.
- 55
56
57
58
59
60

- 1
2
3 Klein, R. 1994. The Problem of Modern Human Origins. In: M. Nitecki & D. Nitecki, *Origins*
4 *of Anatomically Modern Humans* (pp 3–17). New York, Plenum Press, 3–17.
- 5
6 Klein, R., & Scott, K. (1986). Re-analysis of faunal assemblages from the Haua Fteah and
7 other Late Quaternary archaeological sites in Cyrenaican Libya. *Journal of*
8 *Archaeological Science*, 13, 515–542.
- 9
10 Kovda, I., & Mermut, A.R. (2010). Vertic Features. In G. Stoops, V. Marcelino & F. Mees
11 (Eds.), *Interpretation of Micromorphological Features of Soils and Regoliths* (pp. 109–
12 127). Amsterdam: Elsevier.
- 13
14 Kuhn, P., Aguilar, J., Miedema, R. (2010). Textural Features and Related Horizons. In G.
15 Stoops, V. Marcelino & F. Mees (Eds.), *Interpretation of Micromorphological*
16 *Features of Soils and Regoliths* (pp. 217–250). Amsterdam: Elsevier.
- 17
18 Lambeck, K., & Purcell, A. (2005). Sea-level change in the Mediterranean Sea since the LGM:
19 model predictions for tectonically stable areas. *Quaternary Science Reviews*, 24(18–
20 19), 1969–1988.
- 21
22
23 Laville, H. (1976). Deposits in calcareous rockshelters: analytical methods and climatic
24 interpretation. In D.A. Davidson & M.L. Shackley (Eds.), *Geoarchaeology* (pp. 137–
25 155). London: Duckworth.
- 26
27
28 Laville, H., Rigaud, J.-P., & Sackett, J. (1980). *Rockshelters of the Perigord*. London:
29 Academic Press.
- 30
31 Macphail, R.I., & Cruise, G.M. (2001). The soil micromorphologist as team player: A
32 multianalytical approach to the study of European microstratigraphy. In P. Goldberg,
33 V.T. Holliday & C.R. Ferring (Eds.), *Earth Science and Archaeology* (pp. 241–267).
34 New York: Kluwer Academic/Plenum Publishers.
- 35
36
37 Macphail, R.I., & McAvoy, J.M. (2008). A micromorphological analysis of stratigraphic
38 integrity and site formation at Cactus Hill, an early Paleoindian and hypothesized Pre-
39 Clovis occupation in South-Central Virginia, USA. *Geoarchaeology*, 23(5), 675–694.
- 40
41 Macphail, R.I., Goldberg, P., & Linderholm, J. (2000). Geoarchaeological investigations of
42 sediments from Gorham's and Vanguard Caves, Gibraltar: microstratigraphical (soil
43 micromorphological and chemical) signatures In C.B. Stringer, R.N.E. Barton & J.C.
44 Finlayson (Eds.), *Neanderthals on the Edge* (pp. 183–200). Oxford: Oxbow.
- 45
46
47 Macphail, R.I., Cruise, G.M., Allen, M.J., Linderholm, J., & Reynolds, P. (2004).
48 Archaeological soil and pollen analysis of experimental floor deposits; with special
49 reference to Butser Ancient Farm, Hampshire, UK. *Journal of Archaeological Science*,
50 31, 175–191.
- 51
52
53 Mallol, C., Mentzer S.M., Wrinn P.J. (2009). A micromorphological and mineralogical study
54 of site formation processes at the late Pleistocene site of Obi-Rakhmat, Uzbekistan.
55 *Geoarchaeology* 24 (5):548–575.
- 56
57
58
59
60

- 1
2
3 Mallol, C., Hernández, C.M., & Machado, J. (2012). The significance of stratigraphic
4 discontinuities in Iberian Middle-to-Upper Palaeolithic transitional sites. *Quaternary*
5 *International*, 275, 4–13.
- 6
7 Mandel, R.D., & Simmons, A.H. (1997). Geoarchaeology of the Akrotiri Aetokremnos
8 Rockshelter, Southern Cyprus. *Geoarchaeology*, 12(6), 587–605.
- 9
10 McBurney, C.B.M. (1967). *The Haua Fteah (Cyrenaica) and the Stone Age of the South-East*
11 *Mediterranean*. Cambridge: Cambridge University Press.
- 12
13 McBurney, C.B.M., & Hey, R.W. (1955). *Prehistory and Pleistocene Geology in Cyrenaican*
14 *Libya*. Cambridge: Cambridge University Press.
- 15
16 McBurney, C.B.M., Trevor, J.C., & Wells, L.H. (1952). The Haua Fteah Fossil Jaw. *The*
17 *Journal of the Royal Anthropological Institute of Great Britain and Ireland*, 83(1), 71–85.
- 18
19 McBurney, C.B.M., Trevor, J.C., & Wells, L.H. (1953). A Fossil Human Mandible from a
20 Levallois-Mousterian Horizon in Cyrenaica. *Nature*, 172(4385), 889–891.
- 21
22 Mitchell, P. (2016). Africa from MIS 6–2: Where do we go from here? In S.C. Jones & B.A.
23 Stewart (Eds.), *Africa from MIS 6–2: Population dynamics and paleoenvironments* (pp.
24 407–416). Dordrecht: Springer.
- 25
26 MOLAS. (1994). *Archaeological Site Manual* (3rd ed.). London: Museum of London.
- 27
28 Moyer, C. (2003). *The Organisation of Lithic Technology in the Middle and Early Upper*
29 *Palaeolithic Industries at the Haua Fteah, Libya*. Unpublished doctoral dissertation,
30 University of Cambridge, UK.
- 31
32 Muhs, D.R., Budahn, J., Avila, A., Skipp, G., Freeman, J., & Patterson, D. (2010). The role of
33 African dust in the formation of Quaternary soils on Mallorca, Spain and implications
34 for the genesis of Red Mediterranean soils. *Quaternary Science Reviews*, 29, 2518–
35 2543.
- 36
37 Olivieri, A., Achilli, A., Pala, M., Battaglia, V., Fornarino, S., Al-Zahery, N., Scozzari, R.,
38 Cruciani, F., Behar, D.M., Dugoujon, J.M., Coudray, C., Santachiara-Benerecetti, A.S.,
39 Semino, O., Bandelt, H.J., & Torroni, A. (2006). The mtDNA legacy of the Levantine
40 early Upper Palaeolithic in Africa. *Science*, 314(5806), 1767–1770.
- 41
42 Osborne, A.H., Vance, D., Rohling, E.J., Barton, N., Rogerson, M., & Fello, N. (2008). A
43 humid corridor across the Sahara for the migration of early modern humans out of
44 Africa 120,000 years ago. *Proceedings of the National Academy of Sciences*, 105(43),
45 16444–16447.
- 46
47 Pagliai, M., & Stoops, G. (2010). Physical and biological surface crusts and seals. In G.
48 Stoops, V. Marcelino & F. Mees (Eds.), *Interpretation of micromorphological*
49 *characteristics of soils and regoliths* (pp. 419–440). Amsterdam: Elsevier.
- 50
51 Pereira, L., Silva, N.M., Franco-Duarte, R., Fernandes, V., Pereira, J.B., Costa, M.D., Martins,
52 H., Soares, P., Behar, D.M., Richards, M.B., & Macaulay, V. (2010). Population
53
54
55
56
57
58
59
60

- 1
2
3 expansion in the North African late Pleistocene signalled by mitochondrial DNA
4 haplogroup U6. *BMC Evolutionary Biology*, 10, 390.
- 5
6 Powell, A., Shennan, S., & Thomas M.G. (2009). Late Pleistocene demography and the
7 appearance of modern human behavior. *Science* 324, 1298–1301.
- 8
9 Prendergast, A.L., Stevens, R.E., O'Connell, T.C., Hill, E.A., Hunt, C.O., & Barker, G.W.
10 (2016). A late Pleistocene refugium in Mediterranean North Africa?
11 Palaeoenvironmental reconstruction from stable isotope analyses of land snail shells
12 (Haua Fteah, Libya). *Quaternary Science Reviews*, 139, 94–109.
- 13
14 Pye, K., & Blott, S. (2004). Particle size analysis of sediments, soils and related particulate
15 materials for forensic purposes using laser granulometry. *Forensic Science*
16 *International*, 144(1), 19–27.
- 17
18 Rabett, R., Farr, L., Hill, E., Hunt, C., Lane, R., Moseley, H., Stimpson, C., & Barker, G.
19 (2013). The Cyrenaican Prehistory Project 2012: the sixth season of excavations in the
20 Haua Fteah cave. *Libyan Studies*, 44, 113–125.
- 21
22 Reade, H., O'Connell, T.C., Barker, G., & Stevens, R.E. (2016). Pleistocene and Holocene
23 palaeoclimates in the Gebel Akhdar (Libya) estimated using herbivore tooth enamel
24 oxygen isotope compositions. *Quaternary International*, 404, 150–162.
- 25
26 Rebollo, N.R., Weiner, S., Brock, F., Meignen, L., Goldberg, P., Belfer-Cohen, A., Bar-Yosef,
27 O., & Boaretto, E. (2011). New radiocarbon dating of the transition from the Middle to
28 the Upper Paleolithic in Kebara Cave, Israel. *Journal of Archaeological Science*, 38(9),
29 2424–2433.
- 30
31 Sampson, C.G. (1967). Coarse granulometric analysis of the Haua Fteah deposits. In C.B.M.
32 McBurney (Ed.), *The Haua Fteah (Cyrenaica) and the Stone Age of the South-East*
33 *Mediterranean* (pp. 50–54). Cambridge: Cambridge University Press.
- 34
35 Sánchez Vizcaíno, A., & Cañabate, M.L. (1999). Identification of activity areas by soil
36 phosphorus and organic matter analysis in two rooms of the Iberian sanctuary “Cerro El
37 Pajarillo”. *Geoarchaeology*, 14, 47–62.
- 38
39 Santisetban, J.I., Mediavilla, R., López-Pamo, E., Dabrio, C.J., Ruiz-Zapata, M.B., Gil García,
40 J., & Martínez-Alfaro, P.E. (2004). Loss on ignition: a qualitative or quantitative
41 method for organic matter and carbonate mineral content in sediments? *Journal of*
42 *Palaeolimnology*, 32, 287–299.
- 43
44 Schuldenrein, J. (1998). Konispol Cave, Southern Albania, and correlations with other Aegean
45 caves occupied in the Late Quaternary. *Geoarchaeology*, 13(5), 501–526.
- 46
47 Schuldenrein, J. (2001). Stratigraphy, Sedimentology and Site formation at Konispol Cave,
48 Southwest Albania. *Geoarchaeology*, 16(5), 559–602.
- 49
50 Simpson, D.J. (2014). *The Palynology of the Haua Fteah, Libya*. Unpublished doctoral
51 dissertation, Queen's University, Belfast.
- 52
53
54
55
56
57
58
59
60

- 1
2
3 Stein, J.K. (1987). Deposits for archaeologists In M.B. Schiffer (Ed.), *Advances in*
4 *Archaeological Method and Theory* (pp. 337–395). San Diego: Academic Press.
5
6 Stein, J.K. (1992). Organic matter in archaeological contexts. In V.T. Holliday (Ed.), *Soils in*
7 *Archaeology: Landscape Evolution and Human Occupation* (pp. 193–216).
8 Washington: Smithsonian Institution Press.
9
10 Stein, J.K. (2001). Archaeological Sediments in Cultural Environments. In J.K. Stein & W.R.
11 Farrand (Eds.), *Sediments in Archaeological Context*. Salt Lake City: University of
12 Utah Press.
13
14 Stern, N. (2008). Time Averaging and the Structure of Late Pleistocene Archaeological
15 Deposits in Southwest Tasmania. In S.J. Holdaway & L. Wandsnider (Eds.), *Time in*
16 *Archaeology: Time Perspectivism Revisited* (pp. 134–178). Salt Lake City: University
17 of Utah Press.
18
19 Sternberg, R.S. (2001). Magnetic properties and archaeomagnetism. In D.R. Brothwell & A.M.
20 Pollard (Eds.), *Handbook of Archaeological Sciences* (pp. 73–80). Chichester: John
21 Wiley & Sons Ltd.
22
23 Stoops, G. (2003). *Guidelines for Analysis and Description of Soil and Regolith Thin Sections*.
24 Madison, Wisconsin: Soil Society of America Inc.
25
26 Thompson, R., & Oldfield, F. (1986). *Environmental Magnetism*. London: Allen & Unwin.
27
28 Timmermann, A., & Friedrich, T. (2016). Late Pleistocene climate drivers of early human
29 migrations. *Nature*, 538, 92–95.
30
31 Tite, M.S., & Mullins, C. (1971). Enhancement of the magnetic susceptibility of soils on
32 archaeological sites. *Archaeometry*, 13(2), 209–219.
33
34 Tjallingii, Claussen, M., Stuut, J.-B., Fohlmeister, J., Jahn, A., Bickert, T., et al. (2008).
35 Coherent high- and low-latitude control of the northwest African hydrological balance.
36 *Nature Geoscience*, 1, 670–675.
37
38 Tobias, P.V. (1967). Appendix 1B: The hominid skeletal remains of Haa Fteah. In: C.B.M.
39 McBurney (Ed.) *The Haa Fteah (Cyrenaica) and the Stone Age of the South-East*
40 *Mediterranean* (pp338–352) Cambridge: Cambridge University Press.
41
42 Trevor, J.C., & Wells, L.H. (1967). Appendix 1A: Preliminary report on the second
43 mandibular fragment from Haa Fteah, Cyrenaica. In: C.B.M. McBurney (Ed.)
44 *The Haa Fteah, Cyrenaica and the Stone Age of the South-East Mediterranean*
45 (pp336–337). Cambridge: Cambridge University Press.
46
47 Tryon, C.A., & Faith, J.T. (2016). A demographic perspective on the Middle to Later Stone
48 Age transition from Nasera rockshelter, Tanzania. *Philosophical Transactions of the*
49 *Royal Society B, Biological Sciences*, 371, 1698.
50
51 Valentin, C. (1991). Surface crusting in two alluvial soils of northern Niger. *Geoderma*, 48,
52 201–222.
53
54
55
56
57
58
59
60

- 1
2
3 Van Peer, P. (1998). The Nile Corridor and the Out-of-Africa Model: An examination of the
4 archaeological record. *Current Anthropology*, 39(2), S115–S140.
- 5
6 Van Peer, P. (2016). Technological Systems, Population Dynamics, and Historical Process in
7 the MSA of Northern Africa. In: S.C. Jones, & B.A. Stewart (Eds) *Africa from MIS 6-2:
8 Population Dynamics and Paleoenvironments (pp147–159)*. Amsterdam: Springer
9 Verlag.
- 10
11 Van Peer, P. & Vermeersch, P.M. (2007). The place of Northeast Africa in the early history of
12 modern humans: new data and interpretations on the Middle Stone Age. In: P. Mellars,
13 K. Boyle, J. Bar-Yosef, C. Stringer, (Eds) *Rethinking the Human Revolution* (pp 187–
14 198). McDonald Institute Monographs. Cambridge: McDonald Institute.
- 15
16 Van Peer, P., Vermeersch, P.M., & Paulissen, E. (2010). *Chert quarrying, lithic technology
17 and a modern human burial at the Palaeolithic site of Taramsa 1, Upper Egypt* (Egyptian
18 Prehistory Monographs No. 5). Leuven: Leuven University Press.
- 19
20 van Vliet-Lanoë, B. (1998). Frost and soils: implications for paleosols, paleoclimates and
21 stratigraphy. *Catena*, 34, 157–183.
- 22
23 van Vliet-Lanoë, B., Coutard, J.-P., Pissart, A. (1984). Structures caused by repeated freezing
24 and thawing in various loamy sediments: a comparison of active, fossil and experimental
25 data. *Earth Surface Processes and Landforms*, 9, 553–565.
- 26
27 Vaquero, M., Alonso, S., García-Catalán, S., García-Hernández, A., Gómez de Soler, B.,
28 Rettig, D., & Soto, M. (2012). Temporal nature and recycling of Upper Paleolithic
29 artifacts: the burned tools from the Molí del Salt site (Vimbodí i Poblet, northeastern
30 Spain). *Journal of Archaeological Science*, 39(8), 2785–2796.
- 31
32 Vermeersch P.M. (2010). Middle and Upper Palaeolithic in the Egyptian Nile Valley. In:
33 Garcea EAA (ed) *South-Eastern Mediterranean Peoples Between 130,000 and 10,000
34 Years Ago*. (pp 66–88). Oxbow, Oxford.
- 35
36 Vermeersch, P.M. & Van Neer, W. (2015). Nile behaviour and late Palaeolithic humans in
37 Upper Egypt during the Late Pleistocene. *Quaternary Science Reviews*, 130, 155–167.
- 38
39 Wainwright, J. (2009). Weathering, soils and slope processes. In J.C. Woodward (Ed.), *The
40 Physical Geography of the Mediterranean* (pp. 169–202). Oxford: Oxford University
41 Press.
- 42
43 West, L.T., Bradford, J.M., & Norton, L.D. (1990). Crust morphology and infiltrability in
44 surface soils from the southeast and midwest USA. In L.A. Douglas (Ed.), *Soil
45 Micromorphology: A Basic and Applied Science. Proceedings of the VIIIth
46 International Working Meeting on Soil Micromorphology, San Antonio, Texas, July
47 1988* (pp. 107–113). Amsterdam: Elsevier.
- 48
49 White, W.B. (2007). Cave sediments and palaeoclimate. *Journal of Cave and Karst Studies*,
50 69(1), 76–93.
- 51
52
53
54
55
56
57
58
59
60

- 1
2
3 Woodward J.C. (1997a) Late Pleistocene Rockshelter Sedimentation at Klithi. In: Bailey GN
4 (ed) *Klithi: Palaeolithic Settlement and Quaternary Landscapes in Northwest Greece,*
5 *vol 2.* (pp 361–376). Cambridge: McDonald Institute for Archaeological Research.
6
7 Woodward J.C. (1997b) Late Pleistocene Rockshelter Sedimentation at Megalakkos. In: Bailey
8 GN (ed) *Klithi: Palaeolithic Settlement and Quaternary Landscapes in Northwest*
9 *Greece, vol 2.* (pp 377–393) Cambridge: McDonald Institute for Archaeological
10 Research.
11
12 Woodward J.C., & Bailey G.N. (2000) Sediment Sources and Terminal Pleistocene
13 Geomorphological Processes Recorded in Rockshelter Sequences in North-west
14 Greece. In: Foster I.D.L. (ed) *Tracers in Geomorphology* (pp 521–551). John Wiley &
15 Sons, London,
16
17 Woodward, J.C., & Goldberg, P. (2001). The sedimentary records in Mediterranean
18 rockshelters and caves: archives of environmental change. *Geoarchaeology*, 16(4),
19 327–354.
20
21 Yaalon, D.H. (1997). Soils in the Mediterranean region: What makes them different? *Catena*,
22 28, 157–169.
23
24
25
26
27
28
29
30
31
32
33
34
35
36
37
38
39
40
41
42
43
44
45
46
47
48
49
50
51
52
53
54
55
56
57
58
59
60

FIGURES

Figure 1: (a) Location of the CPP study area and the Haua Fteah. Drawing by D. Kemp; (b) Looking East along the northern escarpment of the Gebel Akhdar towards the Haua Fteah. Photo: R. Inglis. (c) View into the Haua Fteah shelter from North. Figure circled for scale. Laser scans of the inside of the cave showing (d) an aerial view and (e) cross-section looking East. Scans: J. Meneely and B. Smith.

Figure 2: Photo of the Middle Trench North-Facing Profile, showing the sedimentological facies distinguished and discussed in this paper. Sediments vary between limestone gravel-dominated facies (Facies 2 and 4) and those with fine, silty sediment (Facies 3 and 5). Note large burning feature extending across the section from the left at the top of Facies Four. Holes from the removal of the first phase of micromorphological sampling are visible ~2.5m from the base of the trench (ranging pole divisions are 50 cm), whilst the holes to the left of the section were made through removal of samples for OSL dating. Photo: G. Barker.

Figure 3: Summary of field facies, existing cultural divisions from McBurney (1967), and dates from Douka et al. (2014).

Figure 4: Profile drawings of the West and North-Facing Profiles showing locations of samples discussed in this paper. Large grey rectangles show location of bulk sedimentological sample columns. Area of new CCP excavations (Trench M) marked in dashed rectangle. Black rectangles mark individual micromorphology samples. Star on West-Facing Profile shows location of Campanian Ignimbrite/Y5 tephra. Section drawings: L. Farr.

Figure 5: Schematic diagram of Facies Five–Three West- and North-Facing Profiles showing relationship between the interpreted site formation processes and bulk sedimentological variables. Where they correspond to micromorphological samples (grey squares), the sediment interpretations are based on micromorphological observations discussed in the text, and where they were not sampled for micromorphological analyses, are based on field observations. Grey lines on bulk sedimentology graphs show mean soil pit values. For colours see online version.

Figure 6: Photomicrographs of key features in the Haua Fteah sediments I: (a) limestone sand and gravel interpreted as roof spall, in silty clay material, PPL (Micro-Fabric 961:2; Context 504; Facies 3 MSA); (b) Stipple- to mosaic-speckled b-fabric, indicating lack of shrink-swelling processes, XPL (Micro-Fabric 939:2; Context 508; Facies 3 MSA); (c) Stipple speckled to micritic crystallitic b-fabric – the micritic calcite may be linked to aeolian deposition, roof spalling, or post-depositional precipitation. XPL (Micro-Fabric 2028:2; Context 521; Facies 5); (d) Micritic and sparitic calcitic precipitation linked to persistent wetting of the sediments, the formation of crystals leading to the development of a platy structure, XPL (Micro-Fabrics 2621:2–4; Context 490; Facies 3 Dabban); (e) dung lenses and fine mineral material laminations marking ephemeral surfaces, PPL (Micro-Fabric 2021:2;

1
2
3 Context 563; Facies 5); and (f) faecal spherulites in dung lens, XPL (Micro-Fabric 2521:2;
4 Context 459; Facies 3 Layer XXV).

5
6 Figure 7: Photomicrographs of key features in the Haua Fteah sediments II: (a) Crust fragments
7 broken through trampling or bioturbation, PPL (Micro-Fabric 939:3; Context 509; Facies 3
8 MSA); (b) 'pedorelict' – fragment of soil potentially trampled into the cave by animals or
9 people (Micro-Fabric 940:2; Context 506; Facies 3 MSA); (c) erosive lower boundary (d)
10 clayey infillings indicating drainage of clay and silt –rich water down-profile, PPL (Micro-
11 Fabric 762:2; PPL; Context 449; Facies 3 LSA); (e) phytolith-rich dung with dendritic
12 manganese nodule, PPL (Micro-Fabric 754A:2; Context 453; Facies 3 LSA) and (f) partially-
13 dissolved bone fragments, indicating diagenesis driven by wetting of the sediments, PPL
14 (Micro-Fabric 754A:2; Context 453; Facies 3 LSA).

15
16 Figure 8: Photomicrographs of anthropogenic features in the Haua Fteah sediments: (a) mixed
17 ash and charred material, PPL (Micro-Fabric 1052:7; Context 535; Facies 3/4 boundary); (b)
18 lens of combustion material (Micro-Fabric 2021:4; Context 568; Facies 5), containing burnt
19 bone, micro-charcoal and ash, and vesicular silica aggregate in overlying Micro-Fabric 2021:5,
20 PPL (Context 563; Facies 5); (c) vesicular silica aggregate, produced through the burning of
21 silica-rich fuel, e.g. grasses PPL (Micro-Fabric 2021:4; Context 568; Facies 5); and d)
22 humified and charred material accumulated on a surface, including angular flint/chert shard,
23 potential knapping debitage, XPL (Micro-Fabric 938:3; Context 522; Facies 5). (e) calcitic
24 wood ash pseudomorphs, PPL (Micro-Fabric 1052:5; Context 513; Facies 4); Calcitic
25 hypocoatings resulting from movement of calcite-rich water, probably from the dissolution of
26 ash, PPL (1052:6; Context 513; Facies 4).

27
28 Figure 9: Particle size distributions of the <2mm non-carbonate fraction of the Haua Fteah
29 sediments (grey) compared to that a sample from a local soil pit (black) and limestone residue
30 (white).
31
32
33
34
35
36
37
38
39
40
41
42
43
44
45
46
47
48
49
50
51
52
53
54
55
56
57
58
59
60

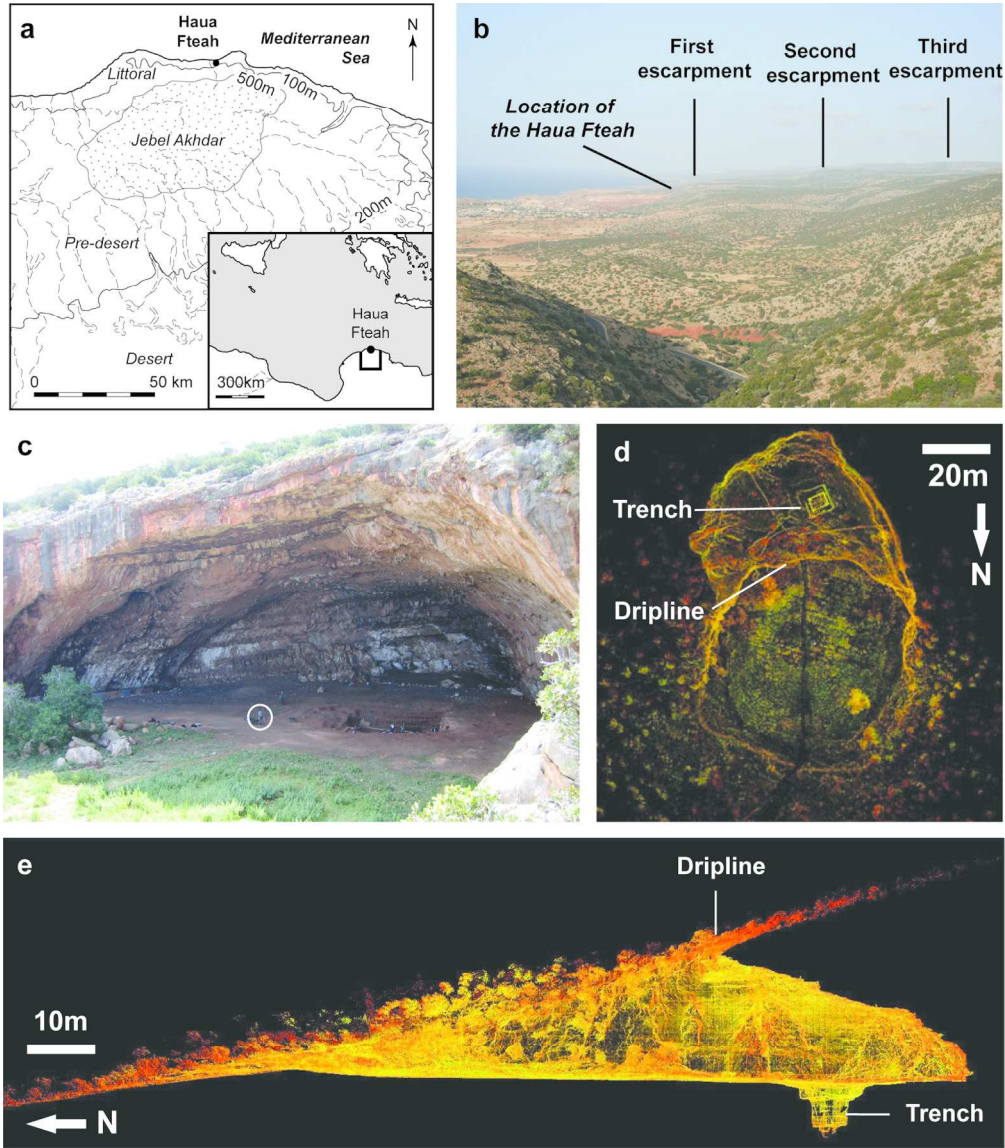


Figure 1: (a) Location of the CPP study area and the Haua Fteah. Drawing by D. Kemp; (b) Looking East along the northern escarpment of the Gebel Akhdar towards the Haua Fteah. Photo: R. Inglis. (c) View into the Haua Fteah from North. Figure circled for scale. Laser scans of the inside of the cave showing (d) an aerial view and (e) cross-section looking East. Scans: J. Meneely and B. Smith.

202x231mm (300 x 300 DPI)



Figure 2: Photo of the Middle Trench North-Facing Profile, showing the sedimentological facies distinguished and discussed in this paper. Sediments vary between limestone gravel-dominated facies (Facies 2 and 4) and those with fine, silty sediment (Facies 3 and 5). Note large burning feature extending across the section from the left at the top of Facies 4. Holes from the removal of the first phase of micromorphological sampling are visible ~ 2.5 m from the base of the trench (ranging pole divisions are 50 cm), whilst the holes to the left of the section were made through removal of samples for OSL dating. Photo: G. Barker.

88x145mm (300 x 300 DPI)

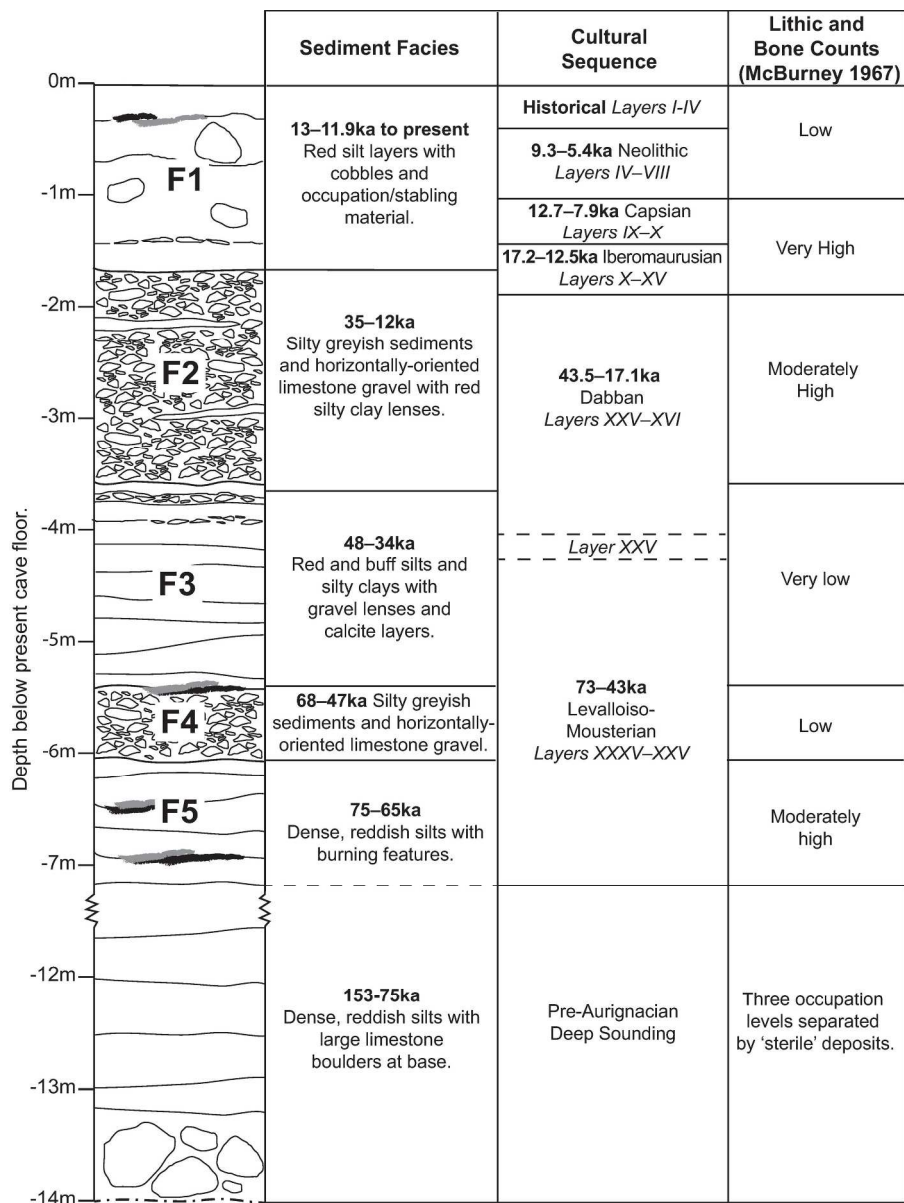


Figure 3: Summary of sedimentological facies, existing cultural divisions from McBurney (1967), and dates from Douka et al. (2014).

208x278mm (300 x 300 DPI)

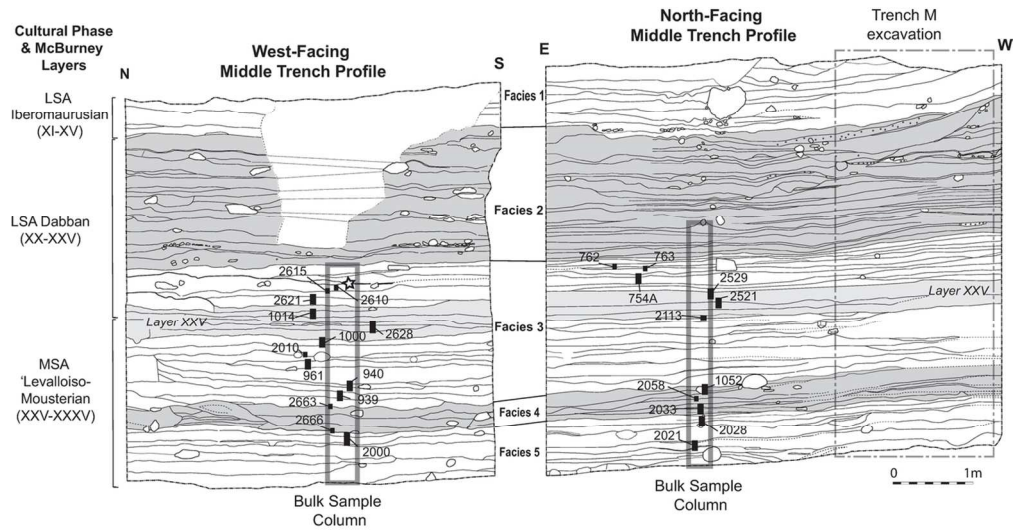


Figure 4: Profile drawings of the West and North-Facing Profiles showing locations of samples discussed in this paper. Large grey rectangles show location of bulk sedimentological sample columns. Area of new CCP excavations (Trench M) marked in dashed rectangle. Black rectangles mark individual micromorphology samples. Star on West-Facing Profile shows location of Campanian Ignimbrite/Y5 tephra. Section drawings: L. Farr.

117x61mm (300 x 300 DPI)

Review

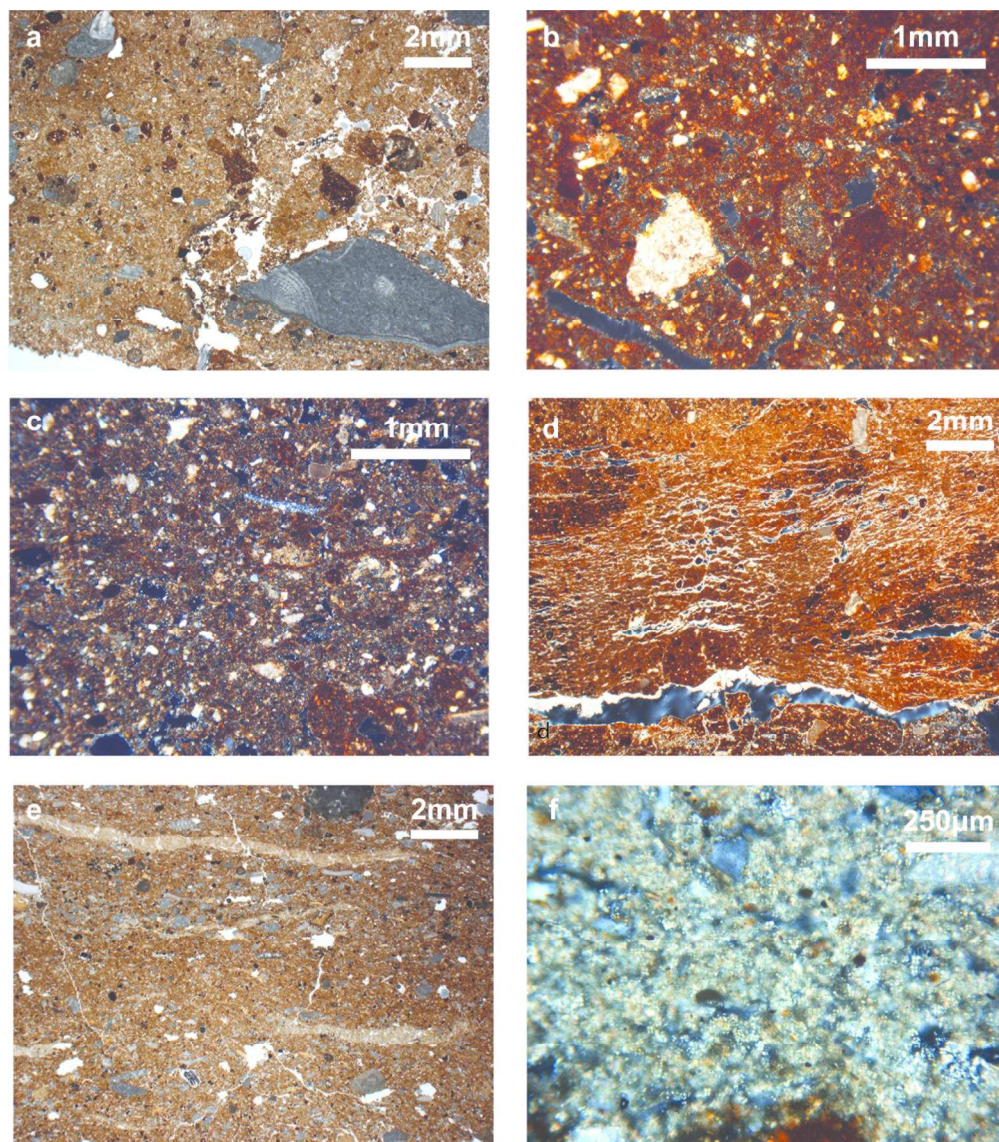


Figure 6: Photomicrographs of key features in the Haui Fteah sediments I: (a) limestone sand and gravel interpreted as roof spall, in silty clay material, PPL (Micro-Fabric 961:2; Context 504; Facies 3 MSA); (b) stipple- to mosaic-speckled b-fabric, indicating lack of shrink-swelling processes, XPL (Micro-Fabric 939:2; Context 508; Facies 3 MSA); (c) stipple speckled to micritic crystallitic b-fabric – the micritic calcite may be linked to aeolian deposition, roof spalling, or post-depositional precipitation. XPL (Micro-Fabric 2028:2; Context 521; Facies 5); (d) micritic and sparitic calcitic precipitation linked to persistent wetting of the sediments, the formation of crystals leading to the development of a platy structure, XPL (Micro-Fabrics 2621:2–4; Context 490; Facies 3 Dabban); (e) dung lenses and fine mineral material laminations marking ephemeral surfaces, PPL (Micro-Fabric 2021:2; Context 563; Facies 5); and (f) faecal spherulites in dung lens, XPL (Micro-Fabric 2521:2; Context 459; Facies 3 Layer XXV).

193x218mm (300 x 300 DPI)

1
2
3
4
5
6
7
8
9
10
11
12
13
14
15
16
17
18
19
20
21
22
23
24
25
26
27
28
29
30
31
32
33
34
35
36
37
38
39
40
41
42
43
44
45
46
47
48
49
50
51
52
53
54
55
56
57
58
59
60

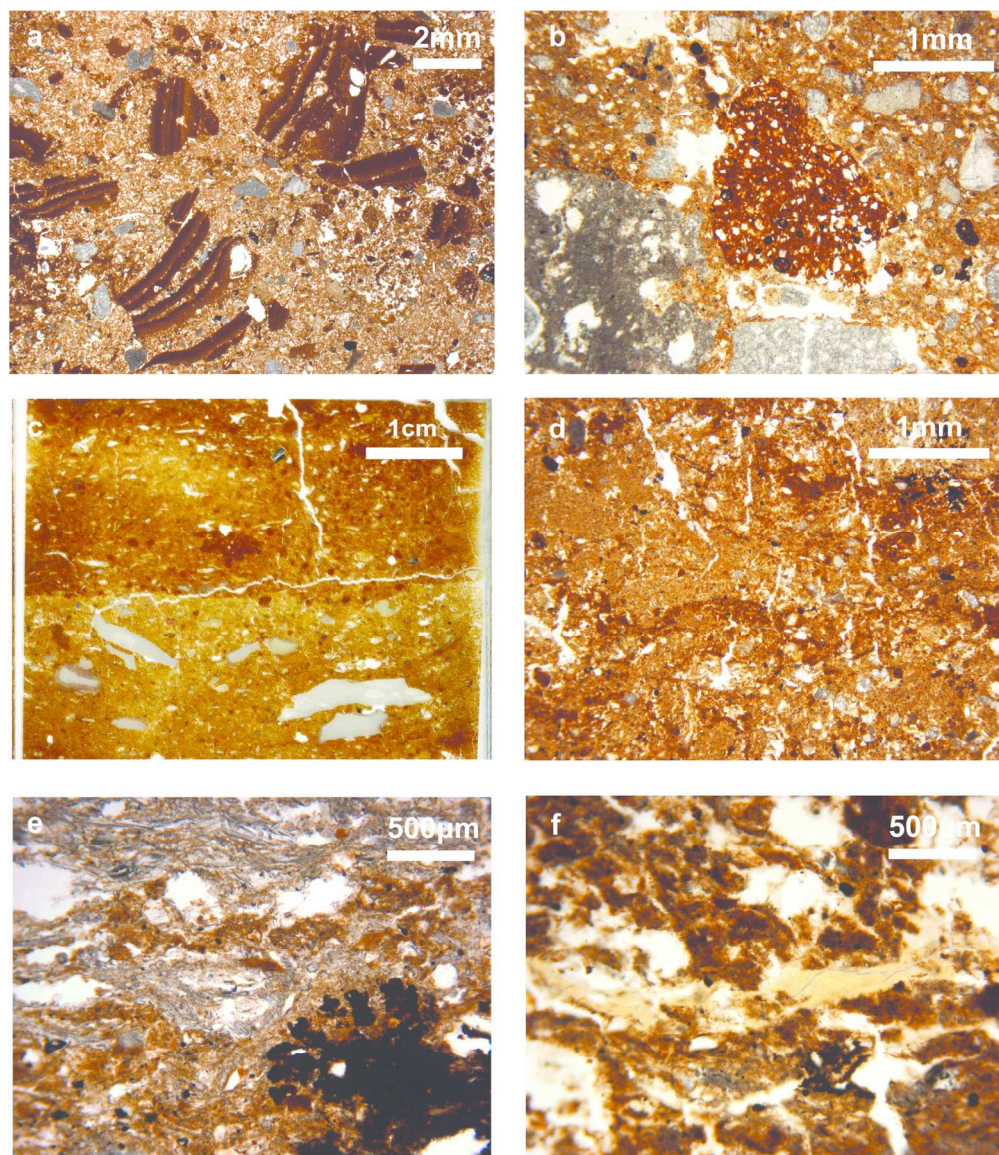


Figure 7: Photomicrographs of key features in the Haula Fteah sediments II: (a) Crust fragments broken through trampling or bioturbation, PPL (Micro-Fabric 939:3; Context 509; Facies 3 MSA); (b) 'pedorelict' – fragment of soil potentially trampled into the cave by animals or people (Micro-Fabric 940:2; Context 506; Facies 3 MSA); (c) erosive lower boundary (d) clayey infillings indicating drainage of clay and silt –rich water down-profile, PPL (Micro-Fabric 762:2; PPL; Context 449; Facies 3 LSA); (e) phytolith-rich dung with dendritic manganese nodule, PPL (Micro-Fabric 754A:2; Context 453; Facies 3 LSA) and (f) partially-dissolved bone fragments, indicating diagenesis driven by wetting of the sediments, PPL (Micro-Fabric 754A:2; Context 453; Facies 3 LSA).

193x221mm (300 x 300 DPI)

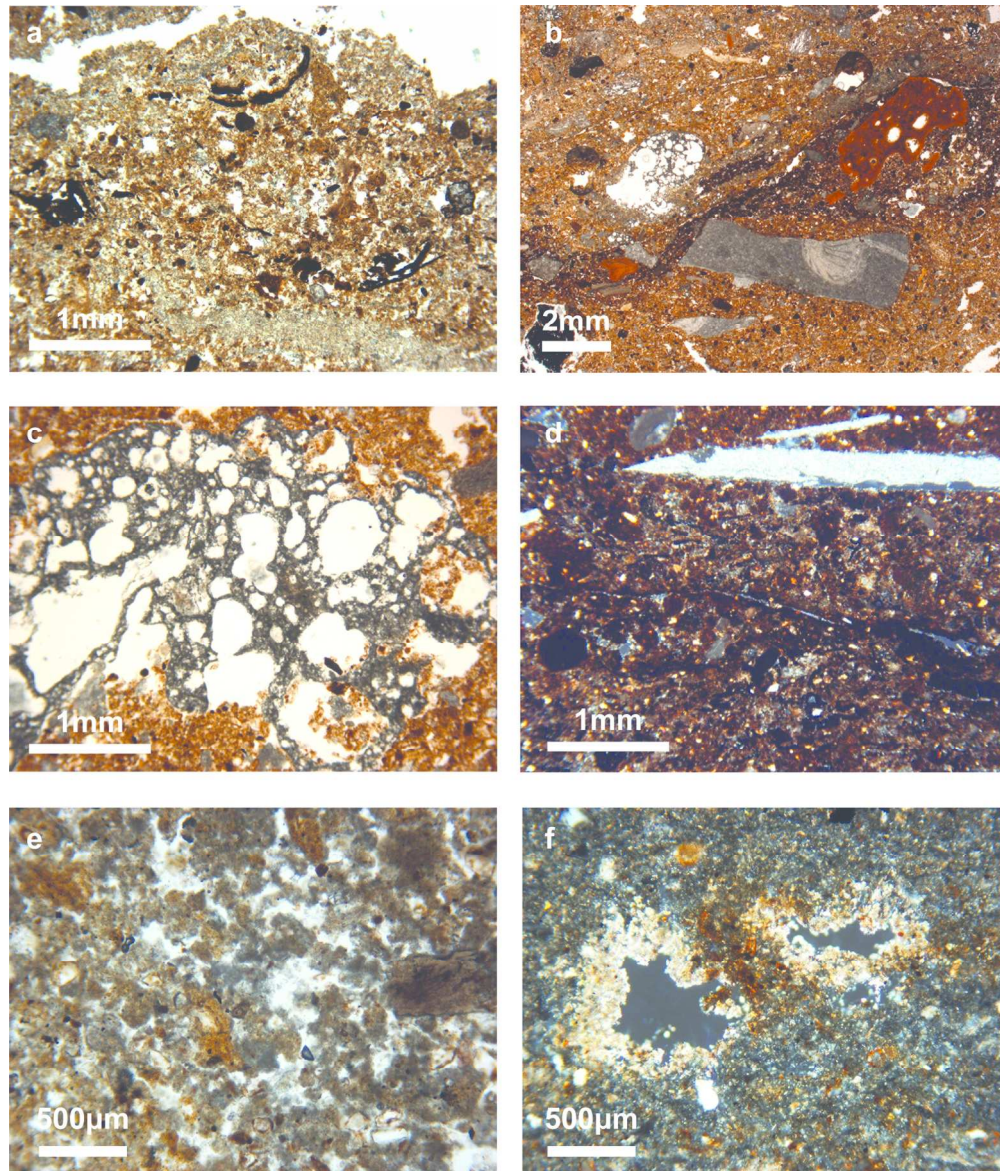


Figure 8: Photomicrographs of anthropogenic features in the Haua Fteah sediments: (a) mixed ash and charred material, PPL (Micro-Fabric 1052:7; Context 535; Facies 3/4 boundary); (b) lens of combustion material (Micro-Fabric 2021:4; Context 568; Facies 5), containing burnt bone, micro-charcoal and ash, and vesicular silica aggregate in overlying Micro-Fabric 2021:5, PPL (Context 563; Facies 5); (c) vesicular silica aggregate, produced through the burning of silica-rich fuel, e.g. grasses PPL (Micro-Fabric 2021:4; Context 568; Facies 5); and d) humified and charred material accumulated on a surface, including angular flint/chert shard, potential knapping debitage, XPL (Micro-Fabric 938:3; Context 522; Facies 5); (e) calcitic wood ash pseudomorphs, PPL (Micro-Fabric 1052:5; Context 513; Facies 4); calcitic hypocoatings resulting from movement of calcite-rich water, probably from the dissolution of ash, PPL (1052:6; Context 513; Facies 4).

194x227mm (300 x 300 DPI)

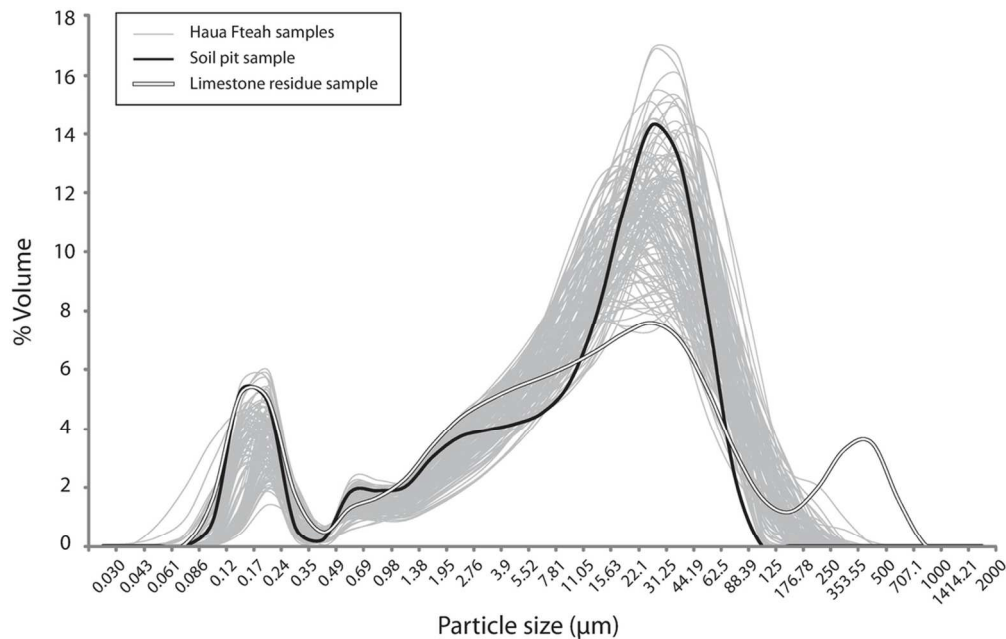


Figure 9: Particle size distributions of the <2mm non-carbonate fraction of the Haua Fteah sediments (grey) compared to that a sample from a local soil pit (black) and limestone residue (white).

103x65mm (300 x 300 DPI)

	Magnetic Susceptibility (m^3kg^{-1})	%LOI (organics)	%CaCO ₃
Soil Pit R			
Sample R2	373.4	5.3	7.8
Sample R3	357.5	5.4	8.1
Soil Pit R Mean	365.45	5.4	8.0
Soil Pit T			
Sample T2	584.0	8.3	8.3
Sample T3	580.6	7.5	8.0
Sample T4	589.8	7.8	8.5
Soil Pit T Mean	584.8	7.9	8.3
Haua Fteah, Facies 5–3			
Mean	321.9	4.0	32.1
Standard Deviation	101.7	0.5	10.5

Table 1: Summary statistics for the soil pit and Haua Fteah Facies 5–3 bulk sedimentological characteristics.